



**MONTCLAIR STATE**  
UNIVERSITY

Montclair State University

**Montclair State University Digital  
Commons**

---

Department of Earth and Environmental Studies Faculty Scholarship and Creative Works Department of Earth and Environmental Studies


---

2015

## Analytical Pyrolysis Principles and Applications to Environmental Science

Michael A. Kruge  
krugem@mail.montclair.edu

Follow this and additional works at: <https://digitalcommons.montclair.edu/earth-environ-studies-facpubs>

 Part of the [Analytical Chemistry Commons](#), [Environmental Chemistry Commons](#), [Environmental Monitoring Commons](#), and the [Geochemistry Commons](#)

---

### MSU Digital Commons Citation

Kruge, Michael A., "Analytical Pyrolysis Principles and Applications to Environmental Science" (2015). *Department of Earth and Environmental Studies Faculty Scholarship and Creative Works*. 66.  
<https://digitalcommons.montclair.edu/earth-environ-studies-facpubs/66>

This Book Chapter is brought to you for free and open access by the Department of Earth and Environmental Studies at Montclair State University Digital Commons. It has been accepted for inclusion in Department of Earth and Environmental Studies Faculty Scholarship and Creative Works by an authorized administrator of Montclair State University Digital Commons. For more information, please contact [digitalcommons@montclair.edu](mailto:digitalcommons@montclair.edu).

Kruger M.A. (2015) Analytical pyrolysis principles and applications to environmental science. In, M. Barbooti, ed., *Environmental Applications of Instrumental Chemical Analysis*. CRC Press, Boca Raton (FL), p. 533-569.

## Chapter 15

### Analytical Pyrolysis Principles and Applications to Environmental Science

*Michael A. Kruger*

#### CONTENTS

- 15.1. Introduction
- 15.2. Pyrolysis-Direct Detection
  - 15.2.1. Rock-Eval Pyrolysis
  - 15.2.2. Pyrolysis-Mass Spectrometry
- 15.3. Pyrolysis-Gas Chromatography
- 15.4. Pyrolysis-Gas Chromatography/Mass Spectrometry
  - 15.4.1. Quantitation and Multivariate Analysis of Py-GC/MS Data
  - 15.4.2. VGI Index
  - 15.4.3. Pyrolytic Marker Compounds for Algal Blooms and Sewage
  - 15.4.4. Analytical Pyrolysis of Airborne Particulate Matter
  - 15.4.5. Analytical Pyrolysis of Spilled Petroleum
- 15.5. Thermochemolysis-Gas Chromatography/Mass Spectrometry
- 15.6. Pyrolysis with Other Detection Systems
- 15.7. Conclusions
- References

#### 15.1. INTRODUCTION

*Pyrolysis* is the heating of organic substances in an inert, oxygen-free atmosphere, thereby avoiding combustion. When performed on a large scale, pyrolysis is involved in industrial processes as diverse as the manufacture of coke from coal and the conversion of biomass into biofuels. In contrast, *analytical pyrolysis* is a laboratory procedure in which small amounts of organic materials undergo thermal treatment, the products of which are subsequently quantified and/or characterized, for example, by gas chromatography. The pyrolysis may be performed “off-line” or “on-line.” In the off-line case, pyrolysis occurs in stand-alone reactor. The pyrolysis products are then extracted or trapped manually prior to further evaluation by chromatographic or other means. In on-line methods, the pyrolysis reactor is coupled directly to the analytical system, be it the injector of a gas chromatograph or a detector such as a flame ionization device or a mass spectrometer, with the pyrolyzate swept along its course by inert carrier gas. In some cases, a trapping mechanism such as cryofocusing is employed, which can permit the use of multiple detection or analytical systems. On-line methods typically only require milligram or even submilligram quantities of sample. Samples may be analyzed with

little pretreatment, thereby minimizing the use of hazardous solvents in the spirit of environmentally conscious “green chemistry.”

Types of samples suitable for analytical pyrolysis include, for example, petroleum source rocks, sediments, soils, biological materials, and artificial polymers. The method is appropriate for macromolecular organic materials of many types, be they “geopolymers” such as kerogen, asphaltenes and humic substances, biopolymers such as proteins and lignin, and manufactured plastics. Such materials are not directly amenable to gas chromatography, so the thermal treatment opens an alternate avenue for molecular analysis.

This chapter primarily focuses on the use of analytical pyrolysis for the chemical characterization of organic contaminants in environmental media, particularly sediments and soils, but also air and water. It presents a variety of instrumental configurations, by which pyrolysis microreactors are directly coupled to detection systems, with or without intervening chromatographic separation of the pyrolyzate. In each instance the chapter provides examples of environmental applications. The pyrolysis terminology employed herein conforms to the IUPAC recommendations [1].

## **15.2. PYROLYSIS-DIRECT DETECTION**

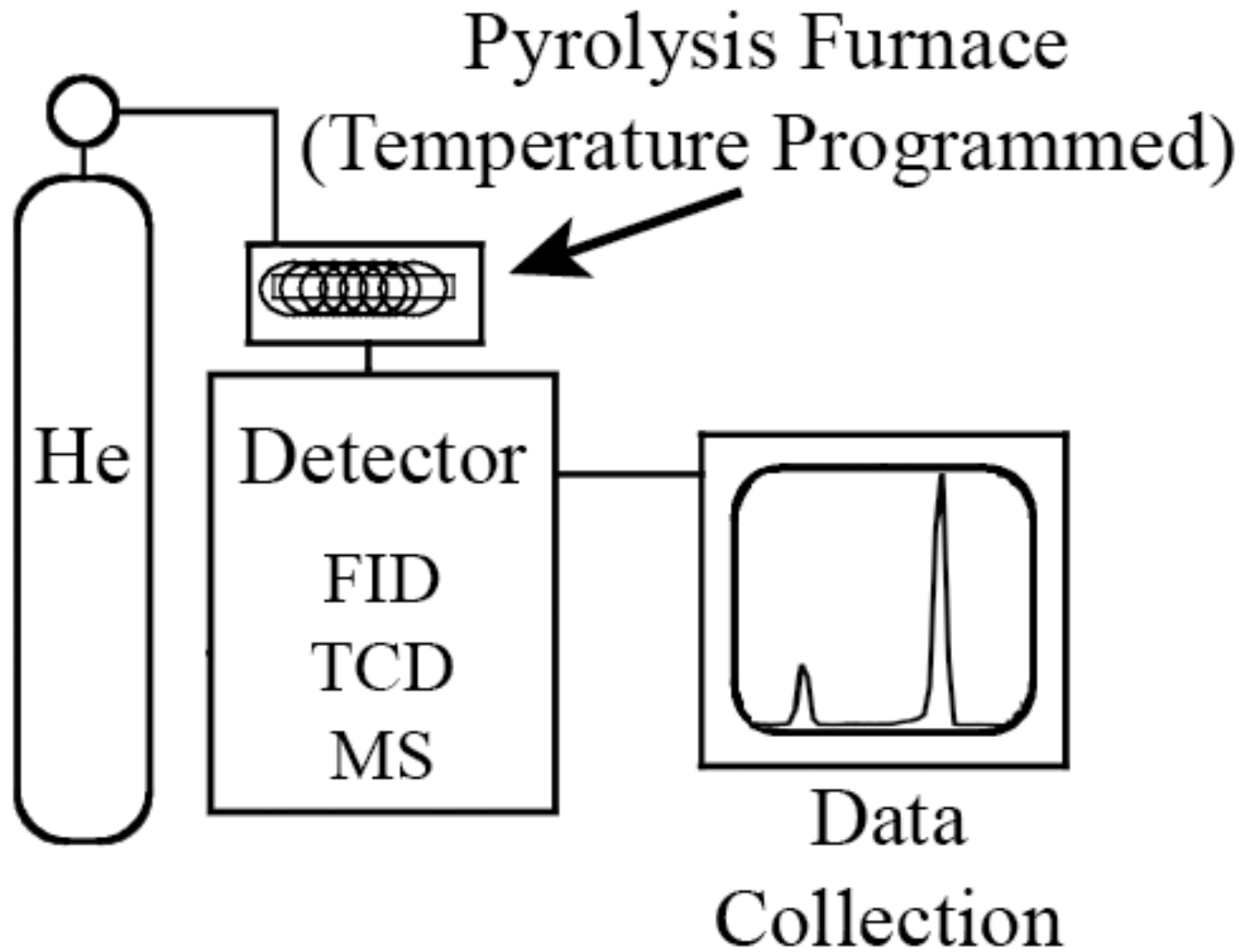
In pyrolysis-direct detection systems, the pyrolysis furnace is coupled to one or more of the detectors typically used in gas chromatographic (GC) systems, but without the intervening GC column. The rapidity of the procedure is its advantage, particularly if bulk characterization is desired. In this configuration, a flame ionization detector (FID), a thermal conductivity detector (TCD), or a mass spectrometer (MS) is commonly employed (Fig. 15.1). The temperature of the pyrolysis furnace may be programmed to gradually increase, allowing the detector to monitor the thermal evolution of the sample.

Pyrolysis systems, be they direct detection or with a coupled chromatograph, may be operated at subpyrolytic temperatures to affect a *thermodesorption* or “thermal extraction” of the sample, by which volatile materials are liberated from the matrix. The sample may then be heated further, at a higher temperature appropriate for true pyrolysis (*stepwise pyrolysis*). Note that if the stepwise approach is not taken and only the higher (true pyrolysis) temperature is employed, the result may likely be a mixture of thermally desorbed and pyrolysis products.

### **15.2.1. Rock-Eval Pyrolysis**

The Rock-Eval pyrolysis system [2–4] is a direct detection instrument widely used in the petroleum industry, most often for the evaluation of petroleum source rock potential. It is an automated device, suitable for the rapid, bulk analysis of multiple samples. Temperature programming is employed to achieve both thermodesorption and stepwise pyrolysis, calibrated quantitatively by external standards. Milligram quantities of crushed rock are placed in a

Figure 15-1. Simplified schematic diagram of a temperature-programmed pyrolysis-direct detection system.



## Pyrolysis - Direct Detection System

crucible, which is then robotically introduced into a furnace preheated typically to 300°C. After being held at the initial temperature for several minutes, the furnace is heated to the final temperature at a prescribed rate (e.g., to 550°C at 25°C min<sup>-1</sup>) where it remains for several minutes before returning to the starting temperature (Fig. 15.2A). During the initial isothermal and subsequent temperature ramp stages, the resulting effluent is delivered to an FID, typically producing two peaks on the pyrogram (Fig. 15.2B). The first peak (S1) corresponds to the yield of thermally desorbed “free hydrocarbons,” while the second peak (S2) is due to the true pyrolysis products, that is, from the high temperature cracking of the kerogen. Carbon dioxide produced during the early portion of the program is trapped and diverted automatically by valves to a thermal conductivity detector (TCD), registering as the S3 peak. The trap is closed at a sufficiently low temperature to exclude CO<sub>2</sub> evolving from the break-down of carbonate minerals, so that the S3 peak is interpreted to represent pyrolytic CO<sub>2</sub> arising from oxygen-bearing functional groups in the organic matter. By using the primary S1, S2, and S3 parameters, along with standard ratios employing them, petroleum source rock richness, quality (the likelihood to generate oil versus gas), and maturity can be readily ascertained [2–4].

While not commonly employed in environmental research, the Rock-Eval instrument has proven itself to be valuable when it has. The method permitted inferences about nutrient inputs and marine productivity in a paleoenvironmental study of Plio-Pleistocene sapropelic sediments in the western Mediterranean Sea [5]. It has also been used to study carbon cycling in modern mangrove sediments [6] and to investigate the association of organic matter with trace metal pollutants in sediments [7, 8].

The Rock-Eval S1 and S2 parameters are useful for initial screening of sediment samples suspected of contamination. For example, organic-rich surface sediment samples from westernmost Lake Ontario, Canada (in this case, defined as those with total organic carbon (TOC) contents in excess of about 2%) show Rock-Eval S2 values above 3 mg pyrolysis yield/g sediment (Fig. 15.3). The sources of organic matter at this location include spilled petroleum and coal, as well as “natural” materials such as aquatic algae, the growth of which was likely enhanced by anthropogenic nutrient inputs [9]. A more extreme organic enrichment was in evidence at the site of an urban sewage sludge spill on the Mediterranean Sea floor off the coast of Barcelona, Spain [10]. The affected sediment is clearly distinguished by Rock-Eval S1 and S2 values above 2 and 4 mg/g, respectively (Fig. 15.3).

The Rock-Eval hydrogen and oxygen indices are among the most widely employed standard parameters produced by this instrument. They are essentially the ratios of S2 to TOC and S3 to TOC, respectively. (Conveniently, the Rock-Eval instrument is commonly configured to also determine TOC.) In the classical interpretation used in petroleum source rock studies, kerogen types I, II and III can be readily recognized on cross-plots of the two indices [2–4] (Fig. 15.4). However, these parameters have also proven their utility in screening samples for

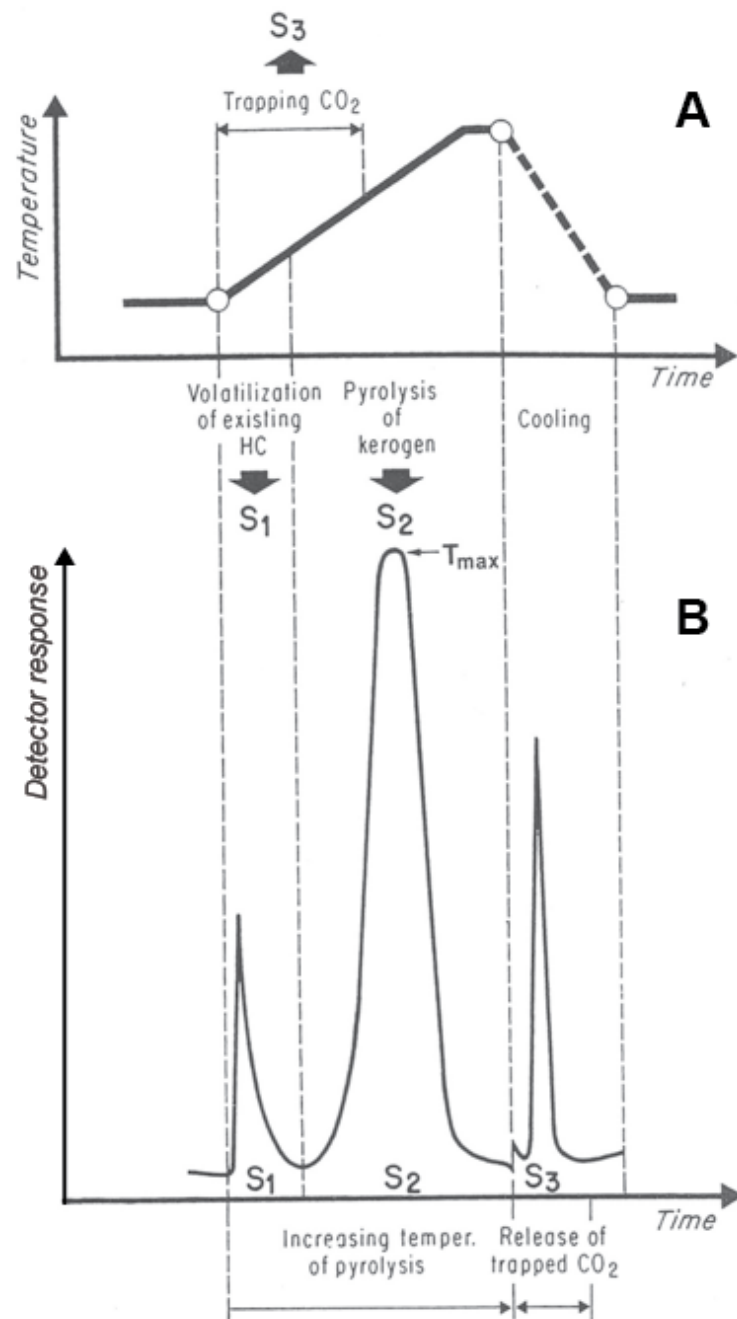


Figure 15-2. Typical Rock-Eval temperature program and resulting pyrogram. (Modified from Ref. 3. Used with permission.)

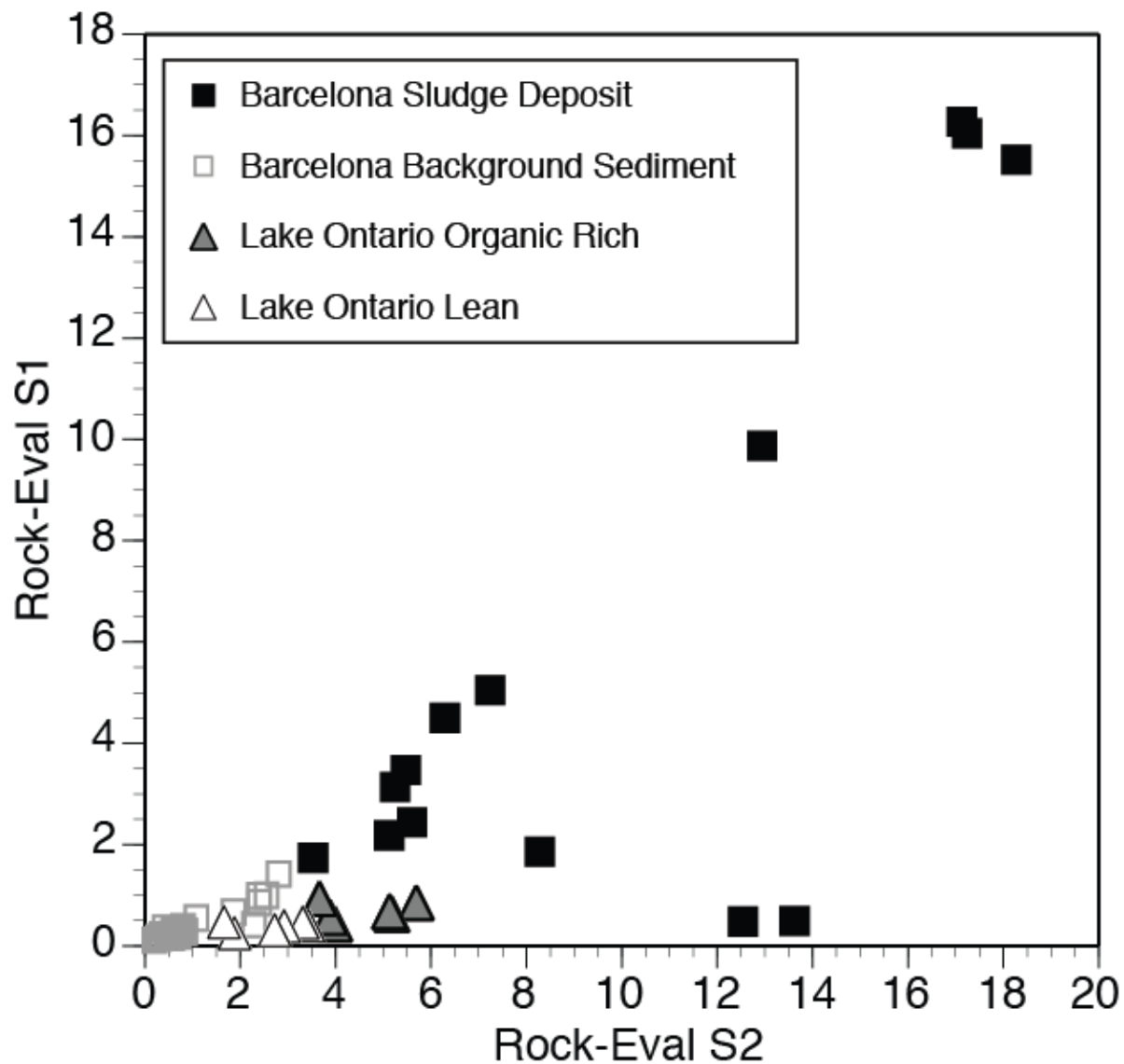


Figure 15-3. Cross-plot of the primary Rock-Eval S1 (mg thermally-desorbed products per gram of sample) and S2 (mg pyrolysis products per gram of sample) parameters as recorded by a flame ionization detector (FID). This illustrates the application of this petroleum prospecting technique to the study of contaminated sediments (data from Refs. 9 and 10).

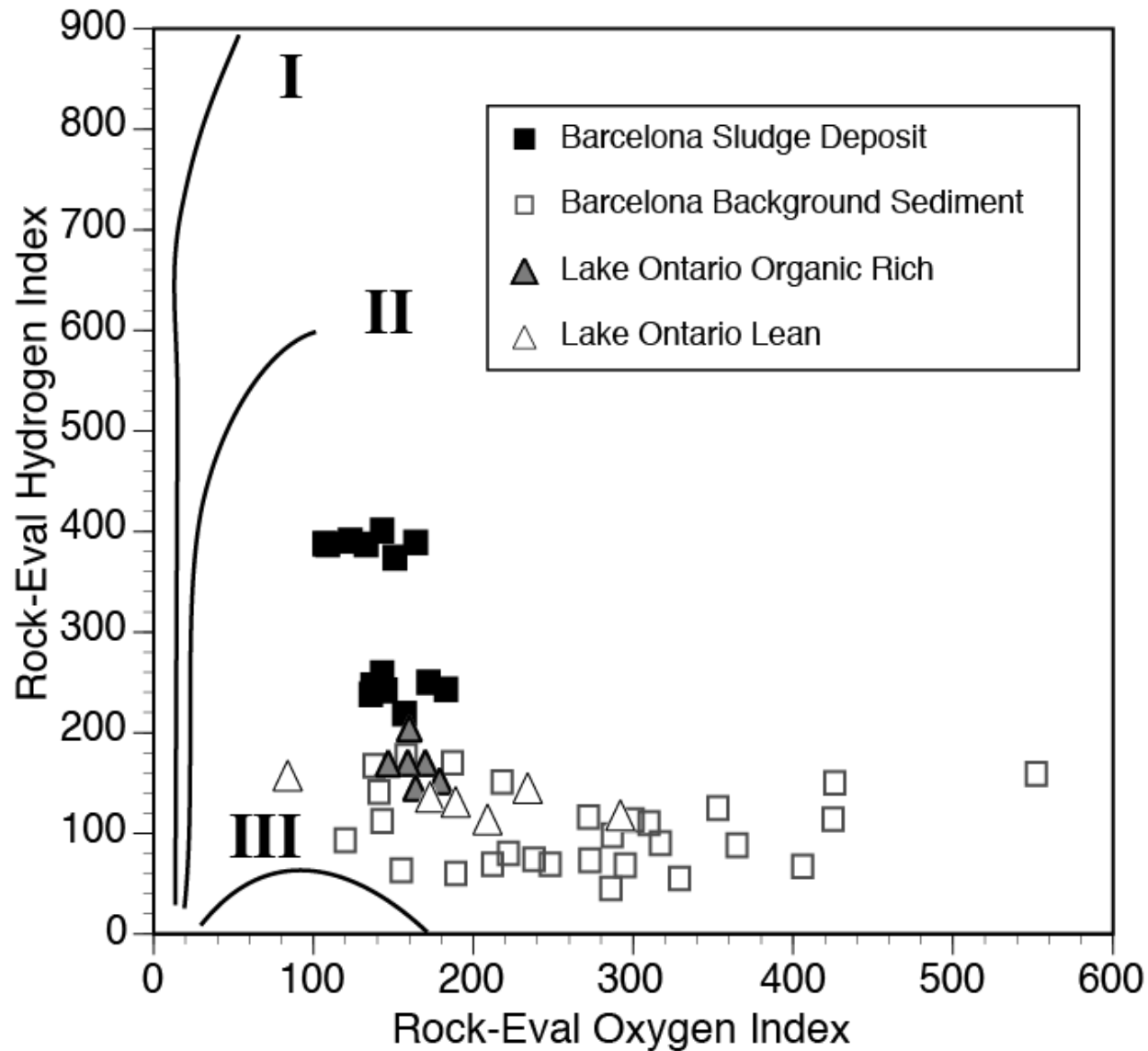


Figure 15-4. Cross-plot of the Rock-Eval Hydrogen Index (mg pyrolysis products/g organic carbon) and Oxygen Index (mg pyrolytic CO<sub>2</sub>/g organic carbon) for the same samples shown in Figure 15-3. These samples plot outside the classic kerogen type ranges (I, II, III) established by Espitalié and others [2] commonly used in petroleum exploration and shown here for reference (data from Refs. 9 and 10).



contamination. The organic-rich sediments and sludge deposits from Lake Ontario and Barcelona mentioned above are clearly distinguished from organic-lean and uncontaminated background sediments by elevated hydrogen index values [9, 10] (Fig. 15.4). While it is interesting to note that organic matter in modern sediments is enriched in oxygen compared to ancient kerogen, the kerogen type designations are neither relevant nor necessary in contamination studies.

### 15.2.2. Pyrolysis-Mass Spectrometry

Another often-used pyrolysis-direct detection configuration employs a mass spectrometer as the detector [11], providing the researcher with some molecular information without sacrificing rapidity of analysis. The Py-MS method has been actively employed since the 1970's and early 1980's [12–14], often in chemotaxonomic studies of microorganisms [15, 16] and in classification of industrial polymers with forensic applications [17]. The resulting mass spectrometric data are typically subjected to multivariate analysis to aid interpretation. A study of the process of peat formation was an early environmental application of Py-MS [18]. Remmler et al. used the similar technique of thermogravimetry/mass spectrometry to observe the desorption of individual polycyclic aromatic hydrocarbons (PAHs) from petrochemical plant sludges and contaminated soils as a function of analysis temperature [19]. As part of a characterization of coal wastewaters, Pörschmann and co-workers analyzed fulvic and humic acids isolated from groundwater by Py-MS [20].

High-resolution mass spectrometry provides an enhanced variant of the Py-MS technique. As with standard Py-MS, it has been used effectively in chemotaxonomic studies of bacteria, with attendant multivariate analysis of the MS data [21]. Field ionization mass spectrometry (FIMS) provides yet another approach, with a “softer” ionization that avoids the molecular fragmentation characteristic of standard electron impact mass spectrometers. As such, a FIMS spectrum of a complex mixture such as a pyrolyzate consists largely of the molecular ions of the constituent compounds (the *molecular ion* being the mass spectral ion indicative of the compound's molecular weight). Py-FIMS systems have been used effectively in detailed molecular investigations of dissolved organic matter in natural waters (Fig. 15.5A) and soil organic matter [22–24]. In a recent advance, pyrolyzers have been coupled with a metastable ion time-of-flight mass spectrometer (Py-MAS-TOF-MS) for the analysis of microbes and microbial lipids in medical [25] and soil [26] studies. The MAS permits better control over ionization and fragmentation than conventional electron ionization, while the TOF-MS has sensitive, rapid spectral acquisition [25]. A low power Py-TOF-MS instrument has been developed with the intention of making it sufficiently robust to travel to the moon to perform lunar soil analyzes [27].

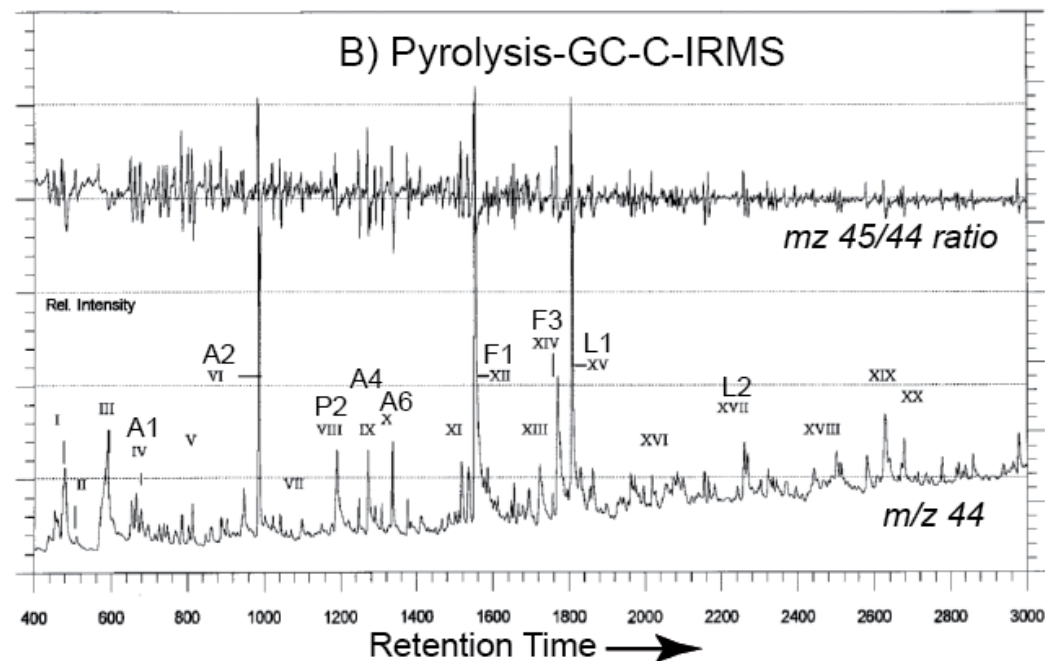
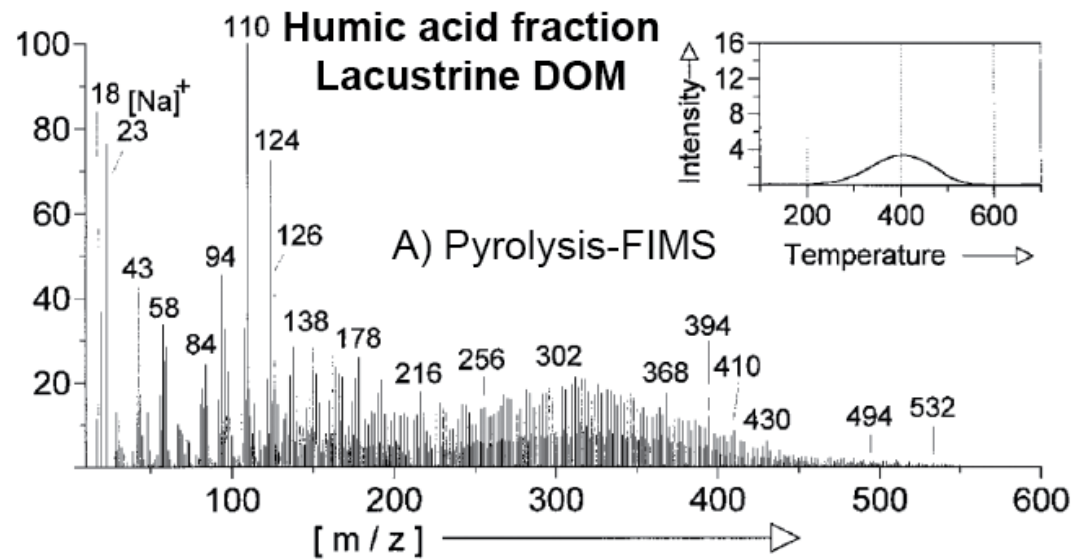


Figure 15-5. Results from the pyrolysis of the humic acid fraction of dissolved organic matter (DOM) in lake water. A) Field ionization mass spectrum of the pyrolyzate with associated profile of pyrolysis yield as a function of temperature. B) The  $m/z$  44 mass chromatogram (lower trace) and corresponding  $m/z$  45/44 ratio from pyrolysis-GC-stable carbon isotope ratio mass spectrometry (C-IRMS). See Table 1 for peak identification. (Modified from Ref. 22. Used with permission.)

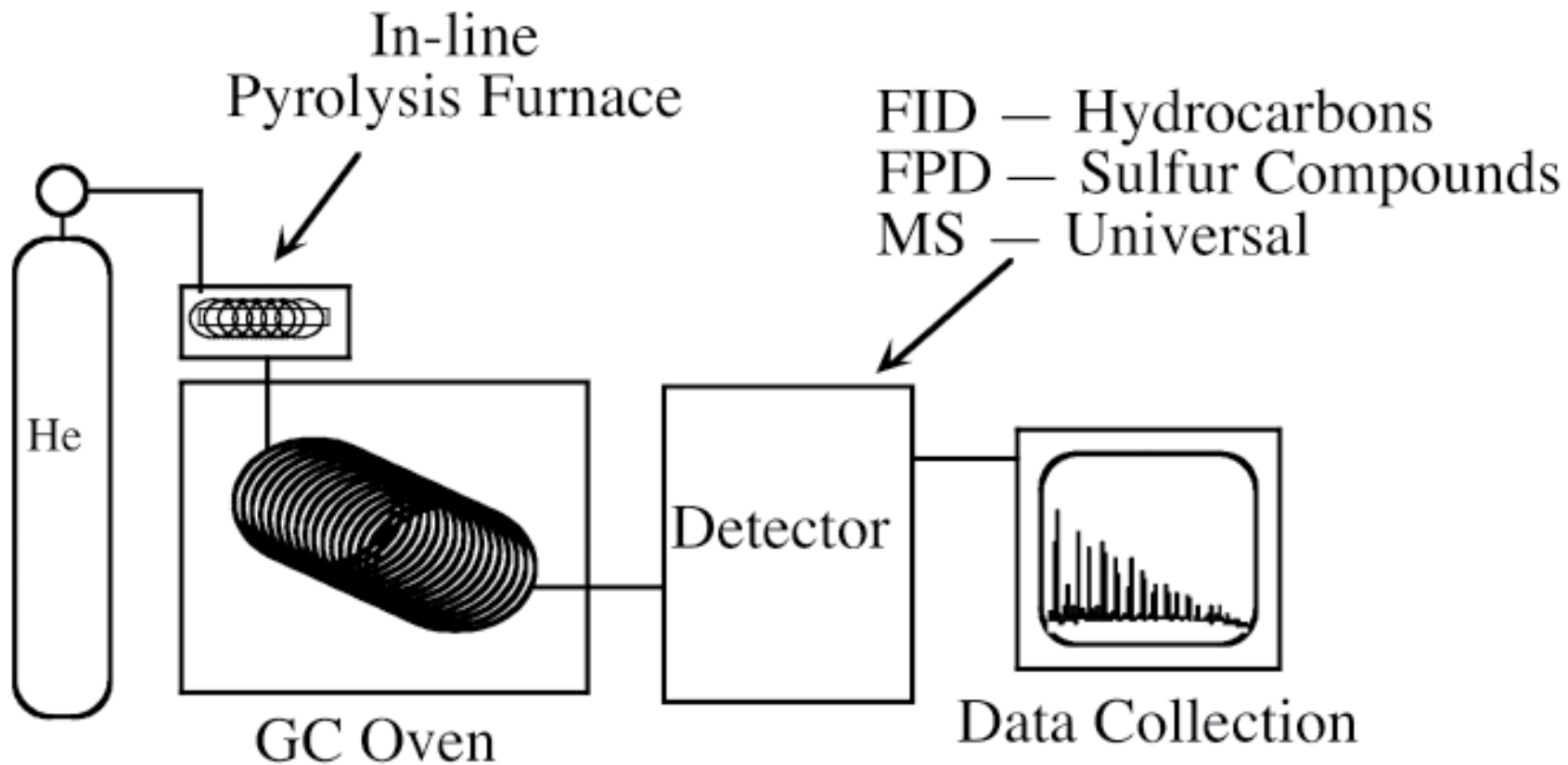
### 15.3. PYROLYSIS-GAS CHROMATOGRAPHY

Analytical pyrolysis is most commonly employed in conjunction with a gas chromatograph (Py-GC), suitable for a wide variety of investigations (e.g., forensic, art appraisal, archeological) of textiles, paints, inks, and biopolymers [28]. In such a system, an in-line pyrolyzer is directly coupled to the GC injector (Fig. 15.6). The chromatograph is commonly equipped with a flame ionization detector (sensitive to hydrocarbons) or a mass spectrometer (discussed separately in Section 15.4). Other devices, such as the sulfur-sensitive flame photometric detector (FPD) and the atomic emission detector (AED), are used less frequently. There are a variety of microscale pyrolyzers available, most notably those with a furnace, with an inductively heated filament (Curie point), and with a resistance coil or ribbon, each with their particular advantages and disadvantages [29, 30].

In 1954, Davison and colleagues were perhaps the earliest to advocate Py-GC as a means for polymer analysis [31]. By 1970, Giraud was applying the method for petroleum source rock characterization [32]. In 1979, Irwin provided a review of the technique and its applications in the first article published in the newly created *Journal of Analytical and Applied Pyrolysis* [33]. At about the same time, Gutteridge compiled a review of Py-GC usage in microbial chemotaxonomy [12] and Dembicki with co-workers described Py-GC methods developed at a major petroleum company for source rock evaluation [34].

The Py-GC technique has proven itself to be useful in evaluating environmental contamination. In an early such study, Whelan et al. [35] subjected contaminated marine sediments to thermodesorption (TD) and stepwise pyrolysis-GC. Peak 1 in Fig. 15.7A denotes the desorbed products liberated from the sediments at about 135°C, subsequently injected automatically into a GC-FID. The resulting chromatogram (Fig. 15.7B) reveals a limited number of identifiable *n*-alkanes and monoaromatic hydrocarbons, as well as what appears to be the chromatographic hump (“unresolved complex mixture” or UCM) characteristic of biodegraded oil. (Refer to Table 15.1 for peak identification.) The sediment sample was then heated to a true pyrolysis temperature of 690°C, producing Peak 2 (Fig. 15.7A) composed of a mixture of aromatic and saturate hydrocarbons lighter than those in Peak 1, without the UCM hump (Fig. 15.7C). Note that Peaks 1 and 2 in this study (Fig. 15.7A) correspond approximately to the Rock-Eval S1 and S2 peaks (Fig. 15.2). The stepwise Py-GC approach is not as rapid as the Rock-Eval method, but some limited molecular data are now available.

Hala undertook a systematic study of contaminated soils in a small abandoned oil field [36], comparing residual oil floating on water in a decrepit wooden holding tank with soil samples collected in the vicinity. He performed Py-GC analysis of solid samples in conjunction with standard GC/MS characterization of the whole oil and solvent extracts of the soil. The conventional extract results showed unsurprisingly that the oil in the tank and contaminated soils was biodegraded, with prominent isoprenoid alkanes and the chromatographic hump due to



## Analytical Pyrolysis - Gas Chromatography System

Figure 15-6. Simplified schematic diagram of an analytical pyrolysis-gas chromatography system. Different detectors may be coupled to the system, including for example, a flame ionization detector (Py-GC-FID), a mass spectrometer (Py-GC/MS), and more rarely, a flame photometric detector (Py-GC-FPD).

Figure 15-7. An early application of thermodesorption- and pyrolysis-GC to the characterization of contaminated sediments. A) FID pyrogram showing product evolution as a function of increasing temperature. The first peak corresponds to thermodesorption products while the second is due to the true pyrolysis products. B) GC trace of the thermodesorbed materials. C) GC trace of the pyrolysis products. See Table 1 for peak identification. (Modified from Ref. 35. Used with permission.)

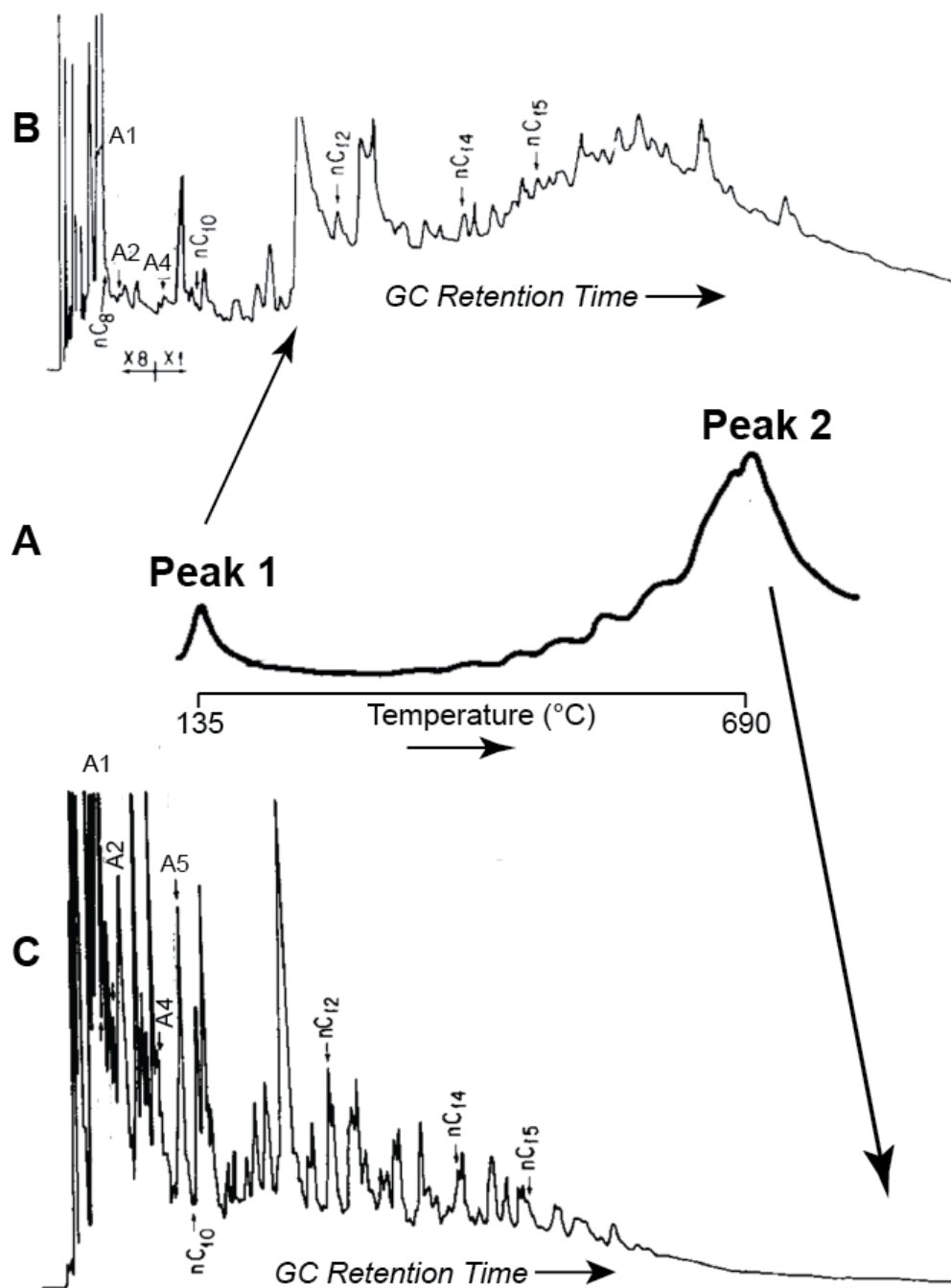


Table 15-1. Peak identification codes for chromatographic figures. Mass spectral base peaks and/or molecular ions are given.

Peak	Compound or isomer group	m/z	Peak	Compound or isomer group	m/z	Peak	Compound or isomer group	m/z
<b>Aromatic compounds</b>			D7	5-phenylundecane	91	N20	n-hexadecanitrile	110
A1	benzene	78	D8	4-phenylundecane	91	N21	n-hexadecanamine, N,N-dimethyl	58
A2	toluene	92	D9	3-phenylundecane	91	N22	n-octadecanitrile	110
A3	ethylbenzene	106	D10	1-phenyldecane	91	N23	n-octadecanamine, N,N-dimethyl	58
A4	13&14-dimethylbenzenes	106	D11	2-phenylundecane	91	N24	n-hexadecamide	59
A5	1,2-dimethylbenzene	106	D12	6-phenyldecane	91	<b>Polysaccharide markers</b>		
A6	styrene	104	D13	5-phenyldecane	91	P1	cyclopentenone	82
A7	C3-alkylbenzene	120	D14	4-phenyldecane	91	P2	furancarboxaldehyde	95
A8	methylstyrene isomer	118	D15	3-phenyldecane	91	P3	methylcyclopentenone	96
A9	indene	116	D16	1-phenyldecane	91	P4	methylfuranone	98
A10	methylindene	130	D17	2-phenyldecane	91	P5	methylfuranocarboxaldehyde	110
A11	naphthalene	128	D18	6-phenyltridecane	91	<b>Sulfur compounds</b>		
A12	2-methylnaphthalene	142	D19	5-phenyltridecane	91	S1	dibenzothiophene	184
A13	1-methylnaphthalene	142	D20	4-phenyltridecane	91	S2	methyl dibenzothiophenes	198
A14	biphenyl	154	D21	3-phenyltridecane	91	S3	dimethyl dibenzothiophenes	212
A15	dimethylnaphthalenes	156	D22	1-phenyldecane	91	S4	trimethyl dibenzothiophenes	226
A16	acenaphthylene	152	D23	2-phenyltridecane	91	S5	benzonaphthothiophene	234
A17	acenaphthene	154	D24	1-phenyltridecane	91	S6	elemental sulfur (S8)	256
A18	methylbiphenyl	168	<b>Phenolic compounds</b>			<b>Steroids</b>		
A19	dibenzofuran	168	F1	phenol	94	\$1	cholestene1	215
A20	trimethylnaphthalenes	170	F2	2-methylphenol	108	\$2	cholestene2	215
A21	fluorene	166	F3	4&3-methylphenols	108	\$3	cholestene3	215
A22	tetramethylnaphthalenes	184	F4	4-ethylphenol	107	\$4	cholestene4	215
A23	phenanthrene	178	F5	vinylphenol	120	\$5	5- $\alpha$ cholestane (20R)	217
A24	anthracene	178	<b>Isoprenoids</b>			\$6	C27 steradiene	215
A25	methylphenanthrenes	192	I1	norpristane	71	\$7	methylcholestene1	215
A26	phenylnaphthalene	204	I2	Pristane	71	\$8	methylcholestene2	215
A27	dimethylphenanthrenes	206	I3	prist-1-ene	69	\$9	methylcholestene3	215
A28	fluoranthene	202	I4	prist-2-ene	69	\$10	methylcholestene4	215
A29	pyrene	202	I5	Phytane	71	\$11	5- $\alpha$ methylcholestane (20R)	217
A30	trimethylphenanthrenes	220	I6	neophytadiene	68	\$12	ethylcholestene1	215
A31	retene	234	I7	phyta-1,3(E)-diene	82	\$13	ethylcholestene2	215
A32	methylpyrene isomers	216	I8	phytol	71	\$14	ethylcholestene3	215
A33	dimethylpyrene isomers	230	I9	unidentified isoprenoid	68	\$15	5- $\alpha$ ethylcholestane (20R)	217
A34	benzo[a]anthracene	228	<b>Methoxyphenols (lignin markers)</b>			\$16	ethylcholestene4	215
A35	chrysene	228	L1	guaiaicol	124	\$17	coprostanol	388
A36	methylchrysene isomers	242	L2	vinylguaiaicol	150	\$18	C29 steradiene	215
A37	dimethyl chrysene	256	<b>Organonitrogen compounds</b>			\$19	C27 stanone	386
A38	benzo[b]fluoranthene	252	N1	pyridine	79	\$20	24-methylsteretraene	378
A39	benzo[j]fluoranthene	252	N2	pyrrole	67	\$21	24-methylsteratriene	380
A40	benzo[k]fluoranthene	252	N3	methylpyridine(a)	93	\$22	24-methylsteradiene	382
A41	benzo[e]pyrene	252	N4	methylpyrrole	80	<b>Tricyclic terpanes</b>		
A42	benzo[a]pyrene	252	N5	C2-alkylpyrrole	94	T1	C23 tricyclic terpane	191
A43	perylene	252	N6	alkyl-alkylidene amine (C8H17N)?	98	T2	C24 tricyclic terpane	191
A44	indeno[1,2,3-cd]pyrene	276	N7	benzonitrile	103	T3	C25 tricyclic terpane	191
A45	benzo[ghi]perylene	276	N8	alkyl-alkylidene amine?	98	T4	C26 tricyclic terpane	191
<b>Carboxylic acids</b>			N9	alkyl-alkylidene amine (C10H21N)	140	T5	C28 tricyclic terpanes	191
C1	CA14 alkanolic acid	73	N10	benzoacetoneitrile	117	T6	C29 tricyclic terpanes	191
C2	hexadecenoic acid	69	N11	piperidinone	98	<b>Hopanes</b>		
C3	CA16 alkanolic acid	73	N12	benzenepropanenitrile	131	H1	18a(H)-trisnorhopane (Ts)	191
<b>Linear alkylbenzenes (LABs)</b>			N13	quinoline	129	H2	17a(H)-trisnorhopane (Tm)	191
D1	5-phenyldecane	91	N14	indole	117	H3	norhopane	191
D2	4-phenyldecane	91	N15	methylindole	131	H4	hopane	191
D3	3-phenyldecane	91	N16	indole dione	147	H5	C31 hopanes	191
D4	1-phenylnonane	91	N17	diketodipyrrole	186	H6	C32 hopanes	191
D5	2-phenyldecane	91	N18	diketopiperazine (Pro-?)	70			
D6	6-phenylundecane	91	N19	carbazole	167			

the unresolved complex mixture of hydrocarbons. The distributions of steranes and terpanes in the tank oil and contaminated soil extracts confirmed their common origin. The extract of the unaffected soil presented almost exclusively the odd carbon-numbered long-chain *n*-alkanes characteristic of natural land plant material [36]. The Py-GC results provided a complementary view (Fig. 15.8). Rather than pyrolyze the whole oil, only its asphaltene fraction was used. This fraction is more resistant to biodegradation and, although a solid, it is nonetheless amenable to microscale pyrolysis. Upon pyrolysis, the oil asphaltene yielded a series of *n*-alkanes from C<sub>4</sub> to at least C<sub>27</sub>, marked with + signs in Fig. 15.8A. The chromatographic resolution here is higher than that depicted in Fig. 15.7, so it is apparent that the *n*-alkanes constitute the second peak in a couplet. The first peak in each pair is the corresponding *n*-alk-1-ene. This is a characteristic of pyrolyzates of aliphatic-rich macromolecules, a phenomenon most readily seen when pyrolyzing artificial polyethylene [28]. Monoaromatic and isoprenoid hydrocarbons are also apparent (Fig. 15.8A). The soil samples were pyrolyzed simply after drying, without solvent extraction. In the strict sense, they yielded a mixture of thermally desorbed compounds and true pyrolysis products. The pyrolyzate of contaminated soil collected near the tank shows a distribution of *n*-alkenes and *n*-alkanes very similar to that of the oil asphaltene (Fig. 15.8A, B), validating the assumption that asphaltene pyrolyzates would be useful for environmental forensic fingerprinting. In addition, the soil yielded a prominent UCM hump, likely indicative of thermally desorbed degraded oil. Aromatic hydrocarbons are relatively more abundant than in the oil asphaltene. Simple phenolic compounds are also apparent in the soil pyrolyzate, a feature not seen in that of the asphaltene. The pyrolyzate of the uncontaminated soil consists primarily simple monoaromatic hydrocarbons and phenols (Fig. 15.8C), likely produced from natural organic matter in the soil. As such, its Py-GC trace is clearly distinguishable from that of the contaminated soil (Fig. 15.8B). The phenolic compounds and at least a portion of the monoaromatic hydrocarbons produced by the contaminated sample are likely also due to admixed natural soil organic matter. Hala found that simple ratios of C<sub>2</sub>-alkylbenzenes (peaks A3, A4, A5) to toluene (A2) and to phenol (F1) correlated positively with the degree of oil contamination of the soil, as determined quantitatively by solvent extraction [36].

#### **15.4. PYROLYSIS-GAS CHROMATOGRAPHY/MASS SPECTROMETRY**

While Py-GC-FID alone was shown to be capable of distinguishing between clean and petroleum-contaminated soils by visual inspection, the complexity of the pyrolyzates precludes much more than rudimentary identification of individual compounds (Figs. 15.7 and 15.8). By reference to external or internal standards or by the recognition of obvious chromatographic elution patterns, a limited number of compounds might be identified on FID traces. The ability of a standard electron impact mass spectrometer to identify unknown compounds is clearly an advantage and thus pyrolysis-gas chromatography/mass spectrometry (Py-GC/MS) has become

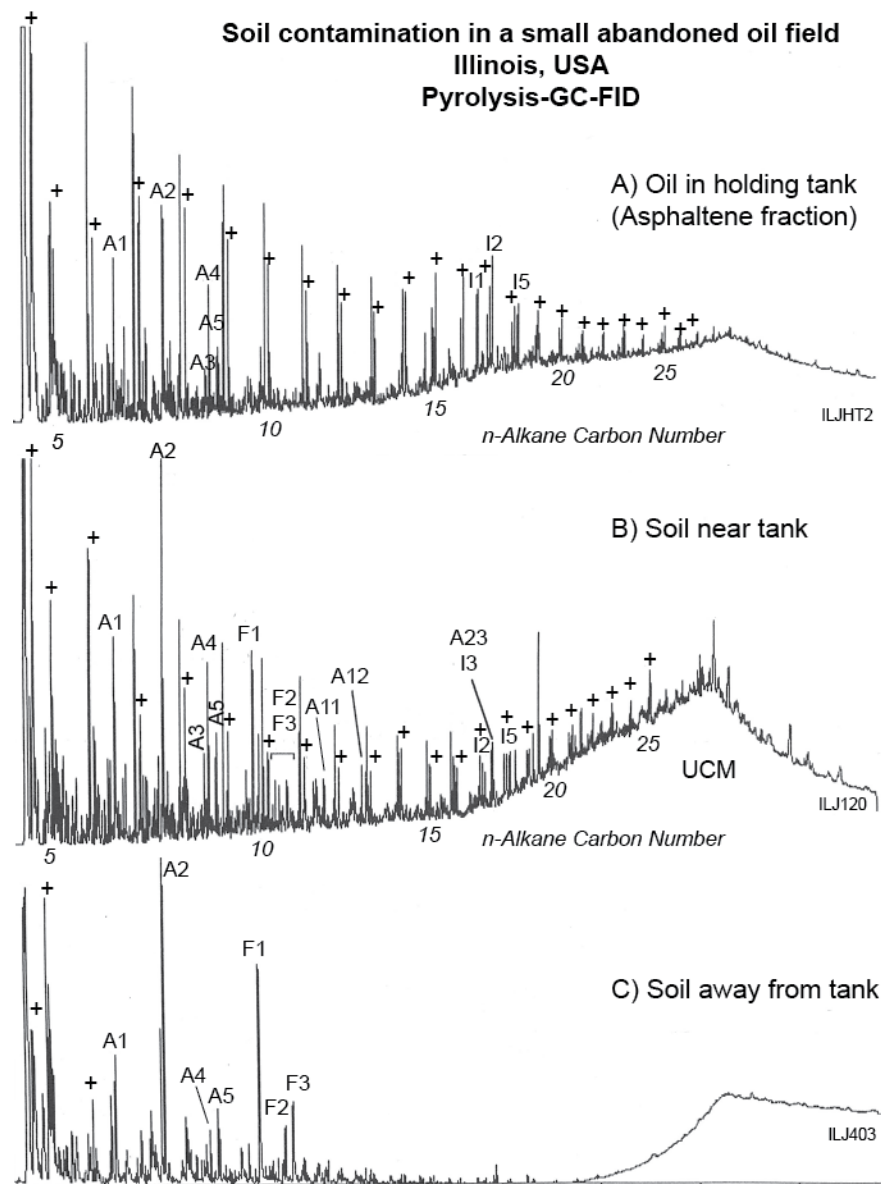


Figure 15-8. Application of pyrolysis-GC-FID to the study of contaminated soil in a small abandoned oil field, central Illinois, USA. A) Asphaltenes of biodegraded oil residues in a holding tank. B) Dried, unextracted soil collected 7 m away from tank. UCM: chromatographically unresolved complex mixture of hydrocarbons characteristic of biodegraded petroleum. C) Dried, unextracted soil collected 17 m away from tank. Coil pyrolysis at 610 °C for 20 s (data from Ref. 36).



the most widely used analytical pyrolysis method in environmental studies. Identification of compounds shown in Fig. 15.8 was in fact facilitated by the reanalysis of a limited number of samples by Py-GC/MS [36].

Py-GC/MS was used in kerogen studies as early as 1975 [37]. In one of the earliest reported environmental applications of Py-GC/MS, de Leeuw et al. [38] used individual ion chromatograms to identify a large number of aromatic compounds in a contaminated soil sample (Fig 15.9). For example, benzo[*a*]anthracene and chrysene (peaks A34, A35) are readily apparent on the *m/z* 228 trace, while barely visible on the total ion current (TIC) chromatogram above. Environmental researchers continued to use both Py-GC and Py-GC/MS, for example, in studies of natural organic matter and petroleum contaminated soils [39] and of urban atmospheric contamination residues on surfaces of buildings [40]. However, Py-GC/MS became the preferred technique, particularly as smaller bench-top mass spectrometers became generally available.

The method has been widely used in studies of soil humus [24, 41, 42] and dissolved organic matter in natural waters [23, 43]. Py-GC/MS was employed to investigate binding of pollutants such as PAHs and petrochemical plant sludges to soil organic matter [19, 44], urban air pollutants on architectural patinas [45], and brown coal dust on various sediment size fractions [46].

Thermodesorption and stepwise pyrolysis-GC/MS proved effective in the characterization of heavily contaminated fluvial sediments from northern Indiana, USA [47]. Selected ion monitoring of the molecular ions of dibenzothiophene and C<sub>1</sub> to C<sub>3</sub>-alkyldibenzothiophenes (peaks S1, S2, S3, S4) produced a chromatogram comparable to the pyrolysis-GC-FPD trace of the same sample (Fig. 15.10A, B). With a study of atmospheric sulfate particulate matter as a rare exception [48], the sulfur-selective FPD is seldom employed with pyrolysis and therefore the flexibility of a mass spectrometer is particularly attractive. In addition to the relatively abundant thermally desorbed thiophenes, the total ion current trace reveals a series of 3- and 4-ring PAHs, notably the methylphenanthrenes, pyrene, and chrysene (peaks A25, A29, and A35 in Fig. 15.10C). After thermodesorption at 310°C for 20 seconds in a coil pyrolyzer, the sample was heated to the true pyrolysis temperature of 610°C, also for 20 seconds. These stepwise pyrolysis products show a shift to relatively more high molecular weight PAHs, in particular the 4- and 5-ring (peaks A35, A36, A39, A41, A42 in Fig. 15.10D). It is likely that these are in fact still thermally desorbed but required higher volatilization temperatures, as was also observed via TD-MS of sludge-contaminated soils [19].

With the understanding that it would likely yield a mixture of thermally desorbed and pyrolysis products, a single analytical run heating the sample at a high temperature (e.g., 610°C for 20 s) may still be advantageous in terms of time and cost savings. This approach effectively detected organic contaminants in harbor sediments from Connecticut, USA (Fig. 15.11). The

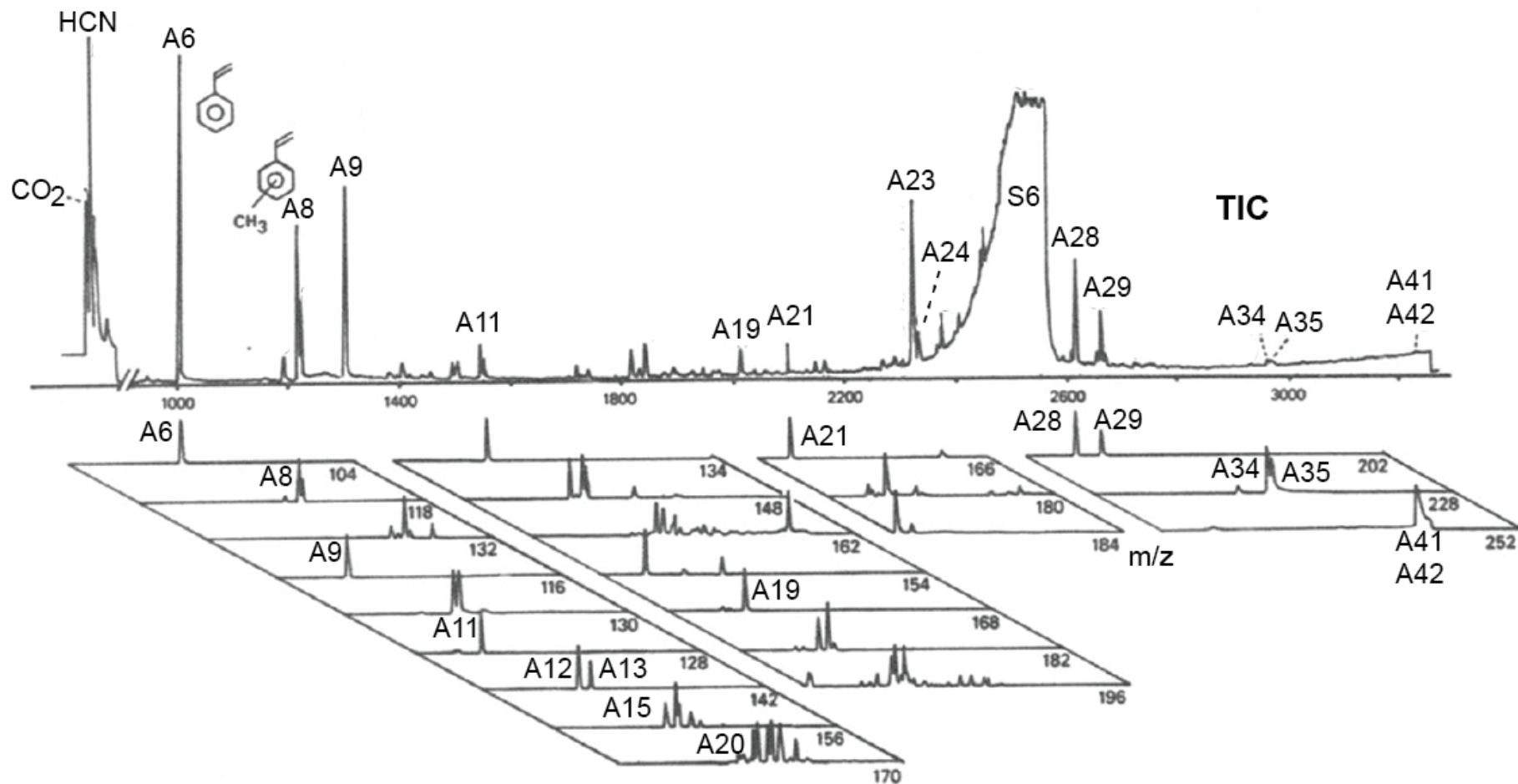
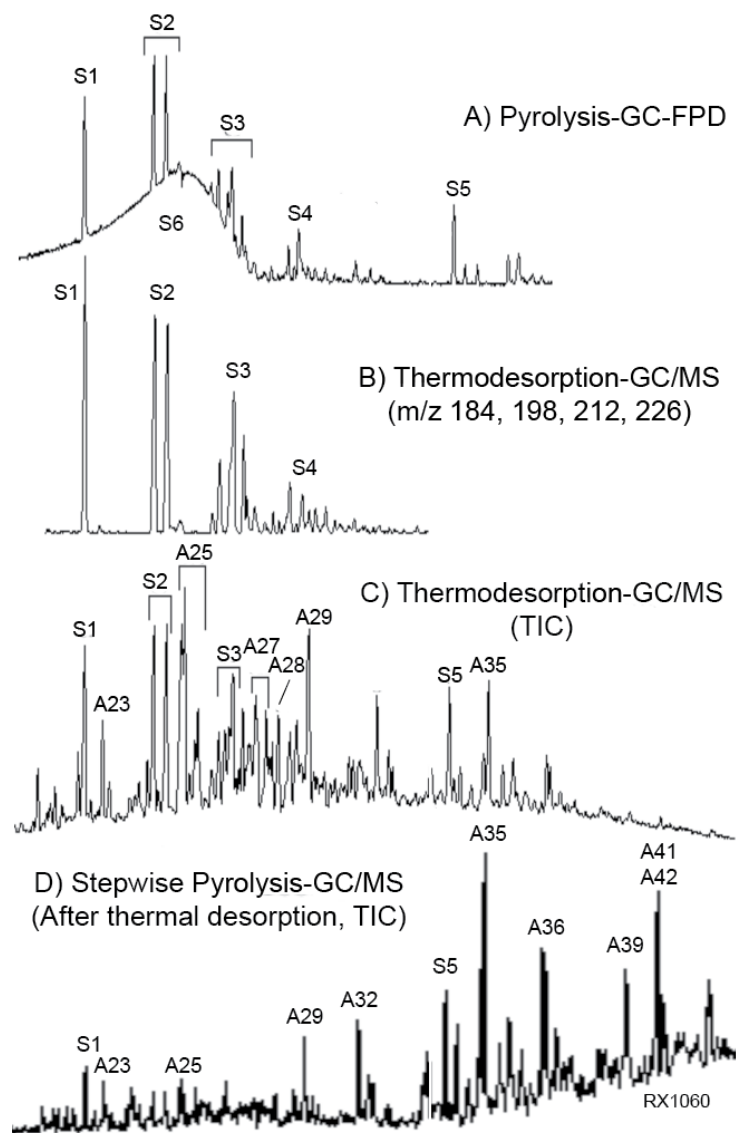


Figure 15-9. An early example of the use of pyrolysis-GC/MS for the analysis of contaminated sediments. The partial mass chromatograms below the TIC trace display the distributions of compounds of interest. See Table 1 for peak identification. (Modified from Ref. 38. Used with permission.)

Figure 15-10. Characterization of aliquots of the same polluted fluvial sediment (West Branch of the Grand Calumet River, Indiana, USA) by a variety of techniques. The retention time range shown in these examples is approximately that of n-C16 to n-C30. See Table 1 for peak identification. A) Distribution of sulfur compounds as revealed by pyrolysis-GC using sulfur-selective flame photometric detection (FPD). B) The (alkyl)dibenzothiophene distribution in the 310 °C thermal desorption product as seen on a mass chromatogram of their summed molecular ions. C) The total ion current trace of the same thermodesorption product showing a predominance of polycyclic aromatic hydrocarbons and thioarenes. D) TIC trace of the products of stepwise pyrolysis at 610 °C after thermodesorption showing a predominance of larger (4- and 5-ring) PAHs (data from Ref. 47).



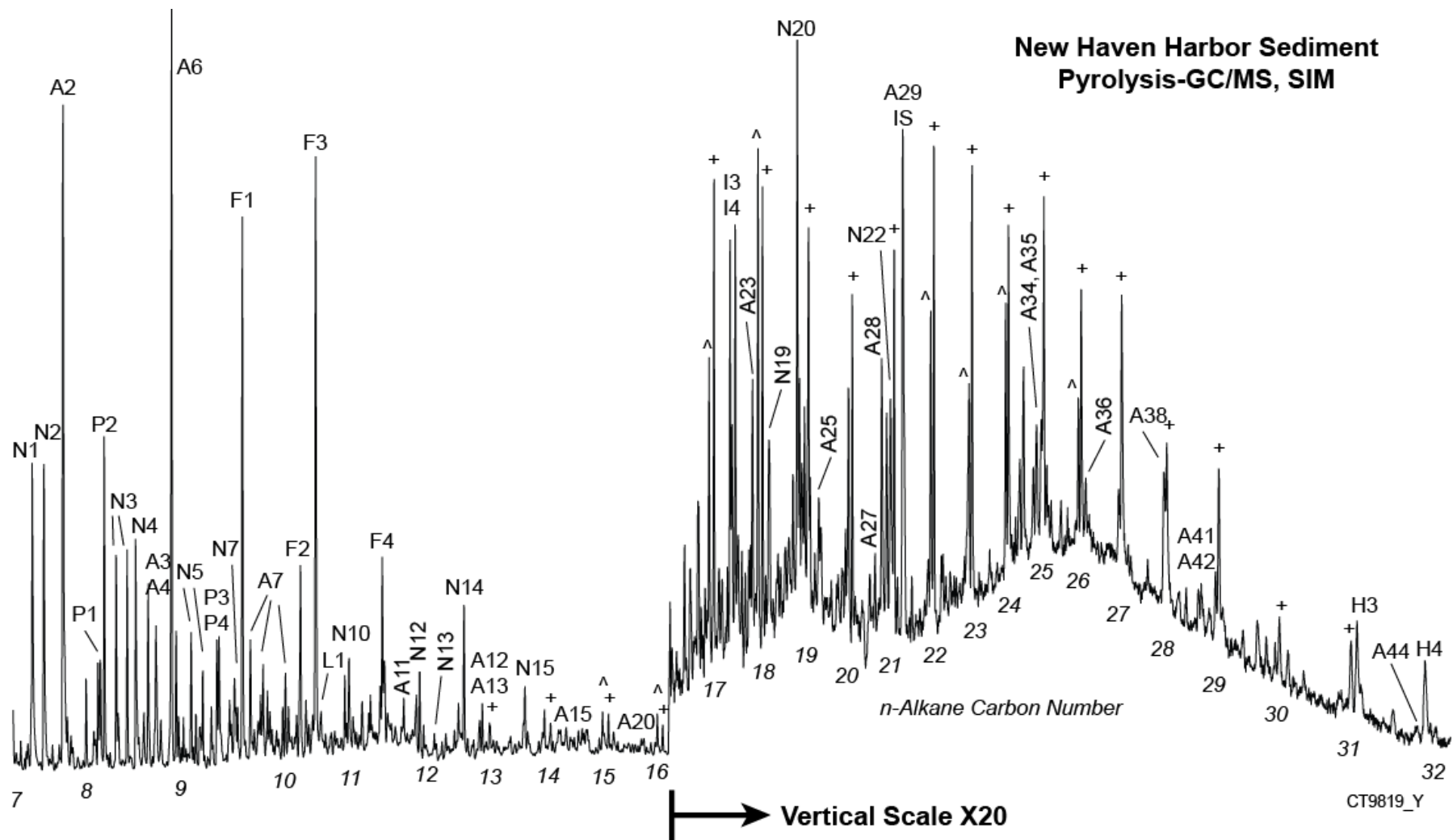


Figure 15-11. Total ion current chromatogram showing pyrolysis products obtained from a harbor sediment sample (New Haven (CT), USA). Data were collected in selected ion monitoring mode employing molecular ions or base peaks of compounds of interest, as determined by prior full scan analysis. See Table 1 for peak identification.

target analytes included acyclic alkanes and alkenes, 2- to 6-ring PAHs, petroleum biomarkers (hopanes), and *n*-alkylnitriles, as well as low molecular weight monoaromatic hydrocarbons, phenolic and nitrogen compounds. After exploratory runs in full scan mode, the analysis was repeated with the mass spectrometer programmed to use only the base peaks of the compounds of interest in selected ion monitoring (SIM) mode, resulting in improved sensitivity and signal-to-noise. The total ion current trace shown is in fact a summation of these purposefully selected ions. A similar approach was employed in experiments with surface sediments from western Lake Ontario, Canada, but with a fast GC temperature ramp of 20°C min<sup>-1</sup>. This shortened the run time considerably, to just 22 minutes, compared to the 80 minutes required for the Connecticut analysis done at 5°C min<sup>-1</sup>. This is advantageous if rapid screening for known contaminants is required. As in the previous example, the low molecular weight compounds generated by pyrolysis of the natural sedimentary organic matter are predominant (Fig. 15.12A). The acyclic hydrocarbon distribution is more clearly evident on the trace of the sum of *m/z* 69 and 71, although the *n*-alkane/alkene doublets are poorly resolved due to the fast GC program (Fig. 15.12B). The main objective, however, was the detection of the PAHs and the 4- to 6-ring parent compounds are indeed readily apparent on their composite mass chromatogram (Fig. 15.12C). This trace was assembled by joining the four constituent mass chromatograms (*m/z* 202, 228, 252, and 276) end-to-end with no overlap and thus provides a compact graphical means to summarize the PAH data.

Munson provided a general overview summarized environmental applications of analytical pyrolysis, with particular attention to Py-GC/MS [49]. Fabbri and others used Py-GC/MS to detect polystyrene, polyvinyl chloride, and other manufactured polymer contamination in the urban lagoonal sediments [50–52]. Work on plastics in environment can be furthered by consulting reference works on their pyrolytic behavior [53, 54]. Kruge and others investigated contamination in Barcelona, Spain harbor sediments [55], while Faure and co-workers used the method to study industrially contaminated fluvial sediments [56, 57].

Mass chromatography is also advantageous when applied to thermodesorption data, formalized as the U.S. Environmental Protection Agency's Method 8275A [58]. The temperature conditions required to effectively thermally desorb hydrocarbon contaminants from petroleum sludges and river sediments have been well documented [19, 56]. In experiments on contaminated fluvial sediment from the Passaic River (New Jersey, USA), thermally desorbed products were analyzed by GC/MS in SIM mode selecting the base peaks of common petroleum biomarkers and polycyclic aromatic compounds (Fig. 15.13A). Mass chromatography permits the visualization of the distributions of the key compounds within each class. The prominent isoprenoids pristane and phytane (peaks I2, I5) and the unresolved complex mixture of hydrocarbons (UCM) seen on the *m/z* 71 trace are the hallmarks of biodegraded petroleum (Fig. 15.13B). Tricyclic terpane and hopane biomarkers on the *m/z* 191 mass chromatogram provide

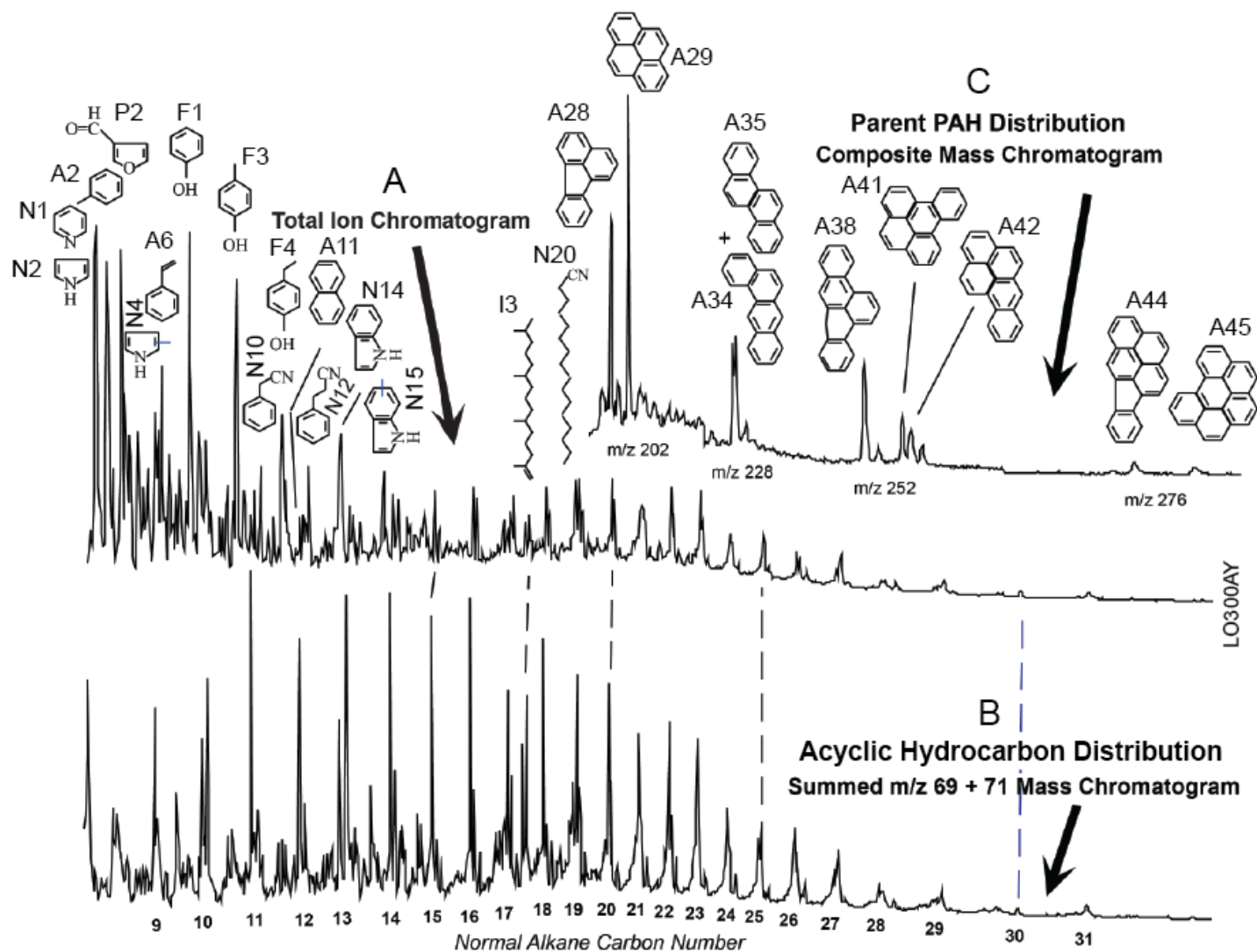


Figure 15-12. Application of pyrolysis-mass chromatography to the study of organic matter in Lake Ontario surface sediments. Data were collected using selected ion monitoring (SIM) of molecular ions and base peaks of major as well as trace constituents known to be present from previous full-scan analyses. The data were collected with a "fast" GC temperature program of 20 °C/min. on a 25 m HP-1 column, such that only 22 minutes of run time were needed. See Table 1 for peak identification. A) Total ion current trace of the selected ions. B) Distribution of normal and isoprenoid alkanes and alk-1-enes on a summed  $m/z$  69 + 71 mass chromatogram. C) Distribution of 4-, 5-, and 6-ring parent PAHs as seen on a composite mass chromatogram of their respective molecular ions ( $m/z$  202, 228, 252, 276). The traces of these four individual ions are linked end-to-end, without overlap or summation.

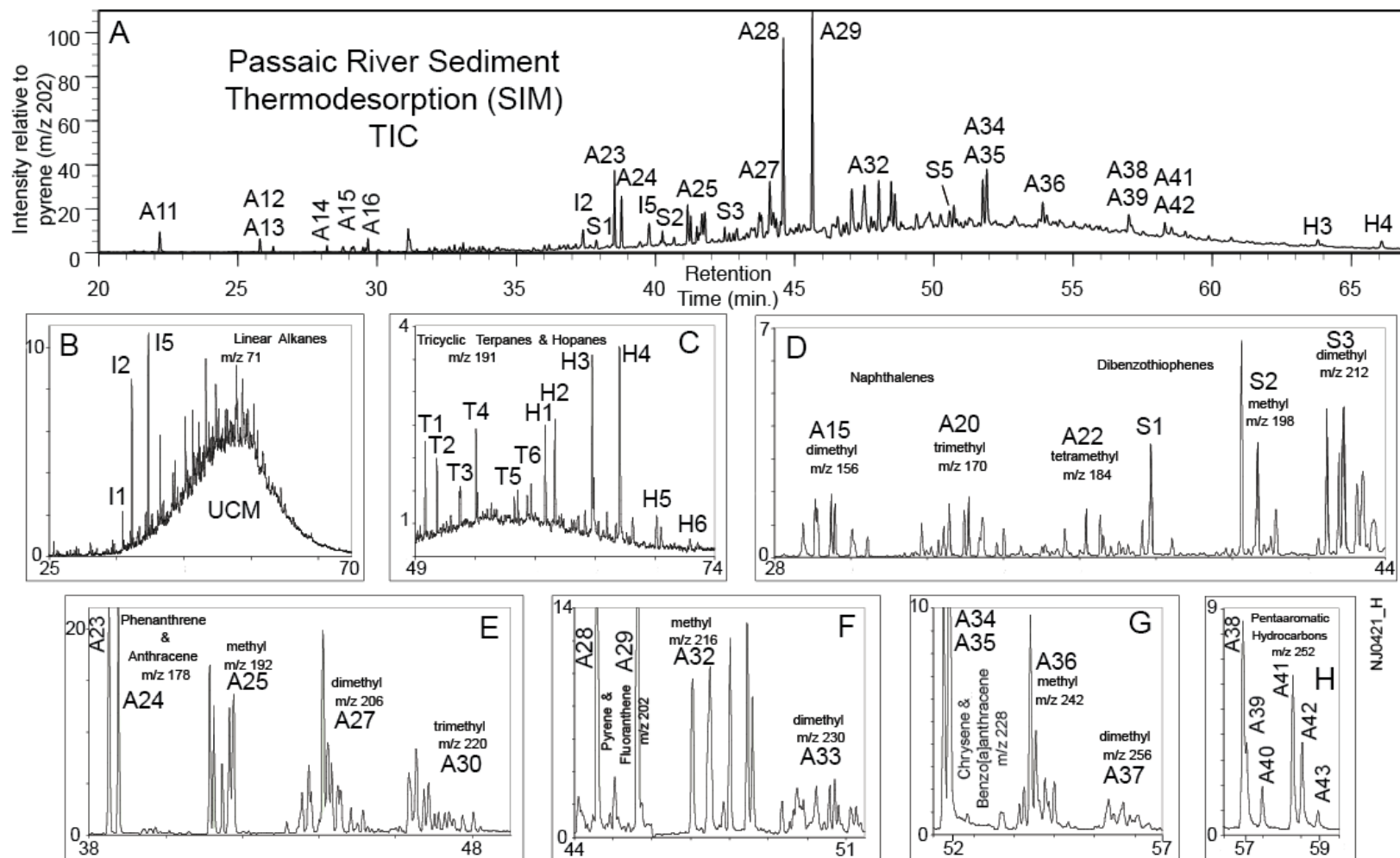


Figure 15-13. Thermodesorption (310 °C, 20 s) GC/MS results from the analysis of contaminated fluvial sediment by selected ion monitoring (Passaic River, Kearny (NJ), USA), using molecular ion or base peaks for compounds of interest chosen after prior full scan analyses. See Table 1 for peak and isomer group identification. A) Total ion current trace summing all ions employed. B) m/z 71 trace showing acyclic alkanes and the "unresolved complex mixture" (UCM). C) m/z 191 trace showing the distribution of tricyclic terpanes and hopanes. D) Composite mass chromatogram (m/z 156, 170, 184, 198, 212) showing the distributions of alkylnaphthalenes and (alkyl)dibenzothiophenes. E) Composite mass chromatogram (m/z 178, 192, 206, 220) showing the distribution of (alkyl)phenanthrenes and anthracenes. F) Composite mass chromatogram (m/z 202, 216, 230) showing the distribution of fluoranthene, pyrene, and alkyipyrene isomers. G) Composite mass chromatogram (m/z 228, 242, 256) showing the distribution of benzo[a]anthracene, chrysene, and alkychrysene isomers. H) m/z 252 mass chromatogram showing the distribution of pentaaromatic hydrocarbons. Composite mass chromatograms display the data for the indicated ions end-to-end, without summation or overlap.

further evidence of petroleum contamination (Fig. 15.13C). The alkylnaphthalene and (alkyl)dibenzothiophene isomer clusters are well-resolved on the composite mass chromatogram constructed from their respective molecular ions (Fig. 15.13D). The same is true for the alkylated phenanthrene/anthracene, pyrene/fluoranthene, and chrysene/benzo[*a*]anthracene series (Figs. 15–13E, F, G) as well as for the parent pentaaromatic hydrocarbons (Fig. 15–13H).

#### 15.4.1. Quantitation and Multivariate Analysis of Py-GC/MS Data

Bar graphs of quantitated chromatographic peak values provide a simpler form of data presentation, particularly useful for a visual comparison of results from several samples. When used for environmental forensic purposes, the members of an isomer cluster (e.g., the dimethylphenanthrenes, marked A27 in Fig. 15.13E) are often summed as a single value upon quantitation [59, 60]. To prepare data for the graphic display, the chromatographic peaks of interest are quantitated using their respective mass chromatograms (e.g., Figs. 15.13B–H). Correction factors (computed from full mass spectra of reference compounds) are then applied for each peak and values normalized for each sample. While environmental forensics practitioners normally use standard solvent extraction methods, data from TD-GC/MS are also amenable to simplified graphical display (Fig. 15.14, Table 15.2). In this figure sample A is the same as the one presented chromatographically in Fig. 15.13, while sample B is sediment collected several kilometers downstream in the same river. This fingerprinting procedure permits ready comparison between the thermal extracts of the two samples, revealing, for example, the relatively higher petroleum biomarker and lower alkylphenanthrene concentrations in sample B.

The various pyrolysis and thermodesorption methods discussed in this chapter are most suitable for inexpensive, rapid sample screening and comparative fingerprinting. However, quantitative analysis is also possible if appropriate internal or external standards are employed, at least for estimation purposes. A long (5 m) sediment core from the Passaic River was subsampled and analyzed by Py-GC/MS, after the addition of a measured amount of perdeuterated pyrene. It was then possible to estimate concentrations of pyrene (thermally desorbed during the single-step run at 610°C) which were found to range between 2 and 30 µg/g sediment, generally increasing with depth (Fig. 15.15). These values are overall less than those achieved using the U. S. Environmental Protection Agency's standard solvent extraction-based methods, but the depth trend is the same (Fig. 15.15). The pyrolysis data were acquired on single samples, whereas the solvent work was performed on composite samples from the same core, in some cases different from those used for pyrolysis. This likely accounts for some of the discrepancy. Buco and others found comparable solvent extraction and pyrolysis quantitation results for parent PAHs in study employing contaminated soil and certified reference materials [61].



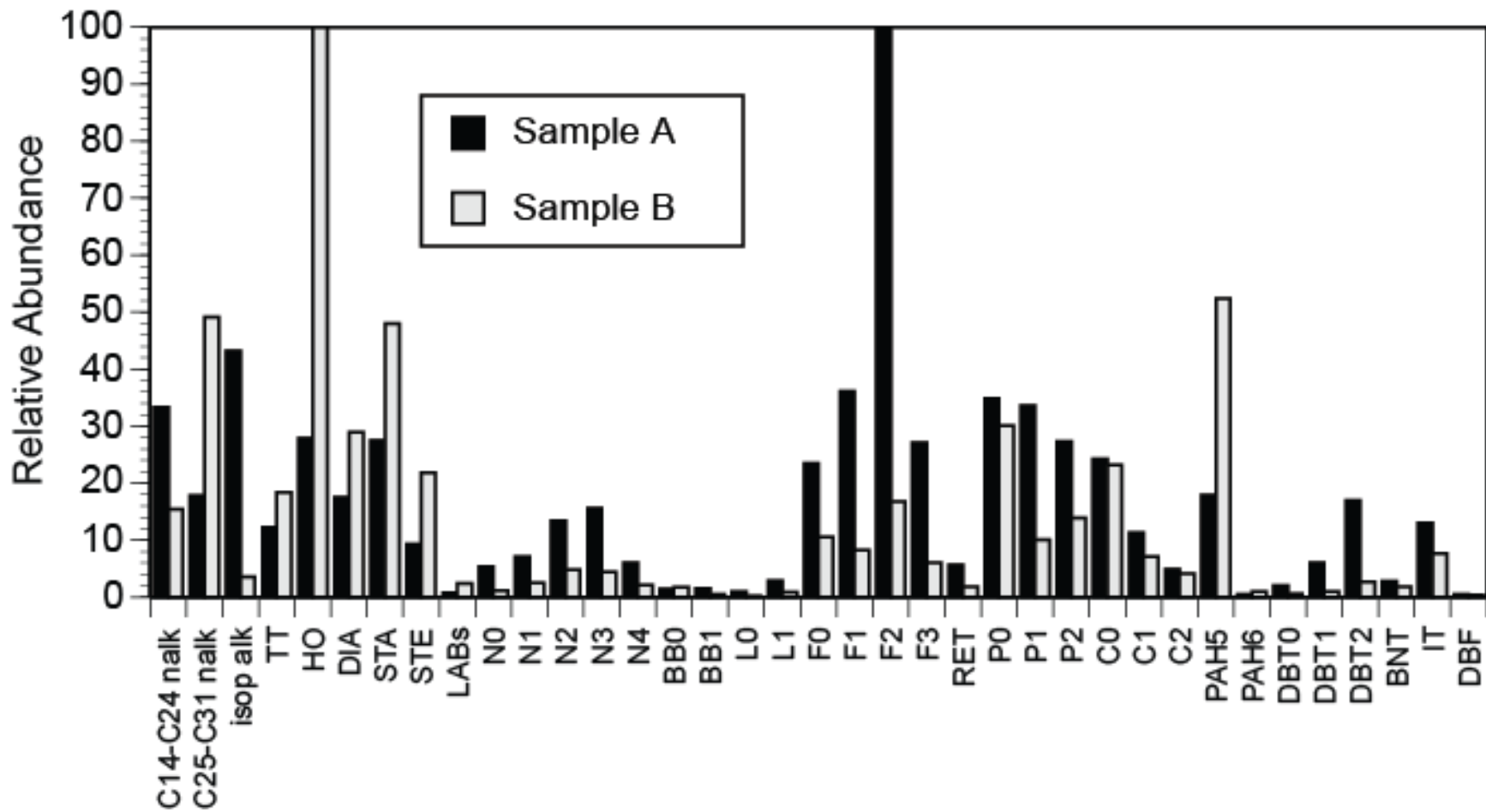


Figure 15-14. Bar graph comparing the distribution of saturate and aromatic thermodesorption products in two contaminated Passaic River sediment samples. Sample A: Kearny (NJ), same as in Figure 15-13. Sample B: Newark (NJ). See Table 2 for compound group codes.

Table 15-2. Compound codes for Figure 15-14.

<b>Code</b>	<b>Compound or isomer group</b>	<b>m/z</b>
C14-C24 nalk	C14 to C24 n-alkanes	71
C25-C31 nalk	C25 to C31 n-alkanes	71
isop alk	Isoprenoid alkanes	71
TT	Tricyclic terpanes	191
HO	Hopanes	191
DIA	Diasteranes	217
STA	Steranes	217
STE	Sterenes	215
LABs	Linear alkylbenzenes	91
N0	Naphthalene	128
N1	Methylnaphthalenes	142
N2	Dimethylnaphthalenes	156
N3	Trimethylnaphthalenes	170
N4	Tetramethylnaphthalenes	184
BB0	Biphenyl	154
BB1	Methylbiphenyls	168
L0	Fluorene	166
L1	Methylfluorenes	180
F0	Phenanthrene & anthracene	178
F1	Methyl phenanthrenes & anthracenes	192
F2	C2-phenanthrenes & anthracenes	206
F3	C3-phenanthrenes & anthracenes	220
RET	Retene	232
P0	Pyrene & fluoranthene	202
P1	Methylpyrene & isomers	216
P2	Dimethylpyrene & isomers	230
C0	Chrysene & benzo[a]anthracene	228
C1	Methylchrysene & isomers	242
C2	Dimethylchrysene & isomers	256
PAH5	Pentaaromatic hydrocarbons	252
PAH6	Hexaaromatic hydrocarbons	276, 278
DBT0	Dibenzothiophene	184
DBT1	Methyldibenzothiophenes	198
DBT2	Dimethyldibenzothiophenes	212
BNT	Benzonaphthothiophene	234
IT	Isoprenoid thiophenes	308
DBF	Dibenzofuran	168

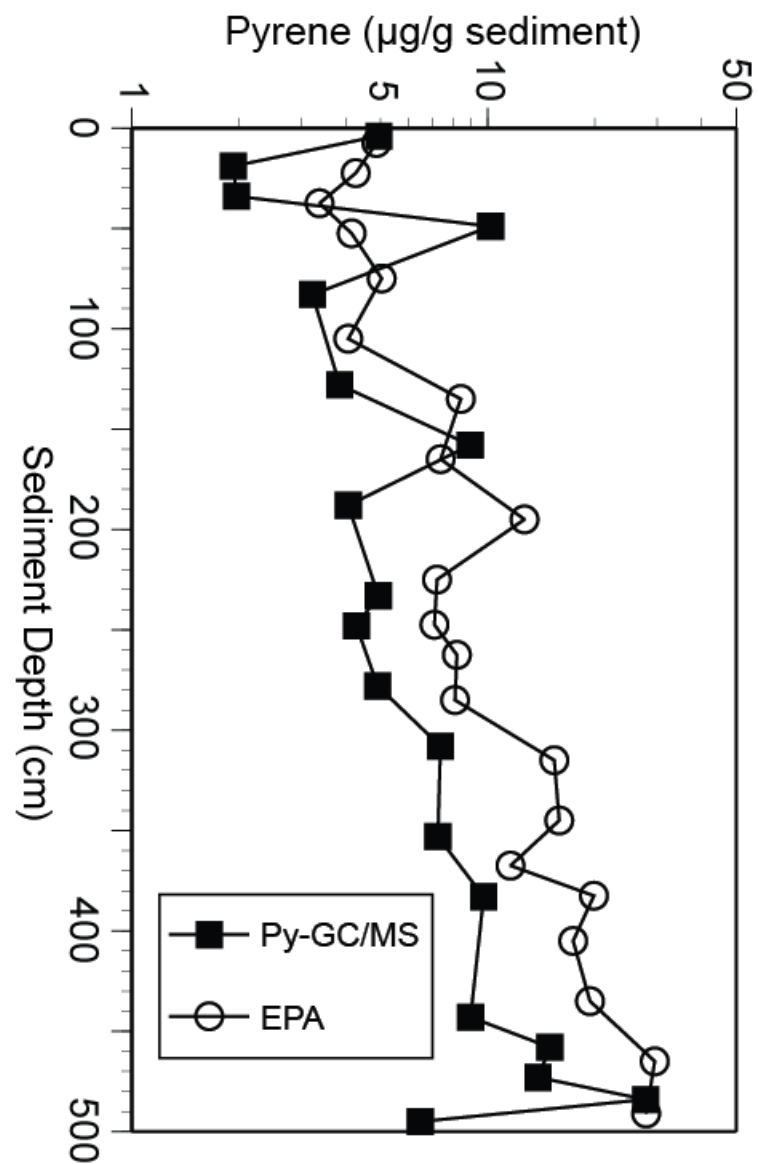


Figure 15-15 Comparison of quantitative results for pyrene concentrations in sediments produced using the standard U.S. Environmental Protection Agency methods for PAH determination and by Py-GC/MS with an internal standard (decadeuteropyrene). Note logarithmic scale. Data are from Lower Passaic River sediment core 7A (data from Ref. 64).

Environmental forensics practitioners often employ multivariate methods when interpreting data produced by classical solvent extraction methods [62, 63]. With the large molecular datasets generated by Py- and TD-GC/MS (e.g., Figs. 15.13 and 15.14), such an approach is equally advantageous. As with the extract data, multivariate methods such as principal components analysis (PCA) can be restricted, if desired, to a suite of compounds of particular interest (such as the PAHs or petroleum biomarkers) detected in the pyrolyzate. In addition, the pyrolysis products of natural organic matter present in the sediment, such as lignin marker and organonitrogen compounds (Table 15.1), can be included to monitor background environmental conditions at the site of investigation. As an example, the Py-GC/MS dataset from the Passaic River sediment core mentioned above (Fig. 15.15) was subjected to PCA. A total of 138 individual compounds and isomer groups (including PAHs, petroleum biomarkers, and pyrolysis products of natural organic matter) were quantitated, normalized, and scaled by taking the square root to dampen wide variations in magnitude. The resulting first principal component accounts for 63% while the second accounts for an additional 21% of the variance in a dataset of 138 variables. Having a total of 84% of the variance in only two composite variables permits a visualization of the essential trends on a simple two-dimensional graph (Fig. 15.16). In this case, high positive values of the first principal component correspond to a greater preponderance of natural organic matter and petroleum contamination in the samples, while negative values indicate relatively greater importance of parent polycyclic aromatic compounds. Although the second principal component is less significant than the first, it adds nuance to the interpretation, with positive values indicative of higher PAH content, while on the negative side it points to a greater influence of terrestrial plant matter. These PCA results reveal a clear stratification within the 5 m long core (Fig. 15.16). The lower portion of the core shows a strong PAH contamination, interpreted to be the legacy of a manufactured gas plant formerly located on the adjacent river bank. A terrestrial vegetation signature is evident in the upper portion of the core, likely reflecting changes in watershed ecology after the decline of the area's heavy industry [64].

#### **15.4.2. VGI Index**

As noted above, natural sedimentary organic matter may derive from terrestrial plant debris washed into bodies of water via runoff or from aquatic organisms such as algae living in the water column. Distinguishing between such allochthonous and autochthonous materials can be important in environmental and sedimentological studies, for which indicators such as the molar C/N and stable carbon isotope ratios are commonly employed [65, 66]. The Vinylguaiacol Indole Index (VGII or "Veggie" Index) was recently proposed as an additional parameter employing Py-GC/MS data [67]. Vinylguaiacol is a methoxyphenol and one of the most abundant pyrolysis products of lignin [68], while the organonitrogen compound indole is

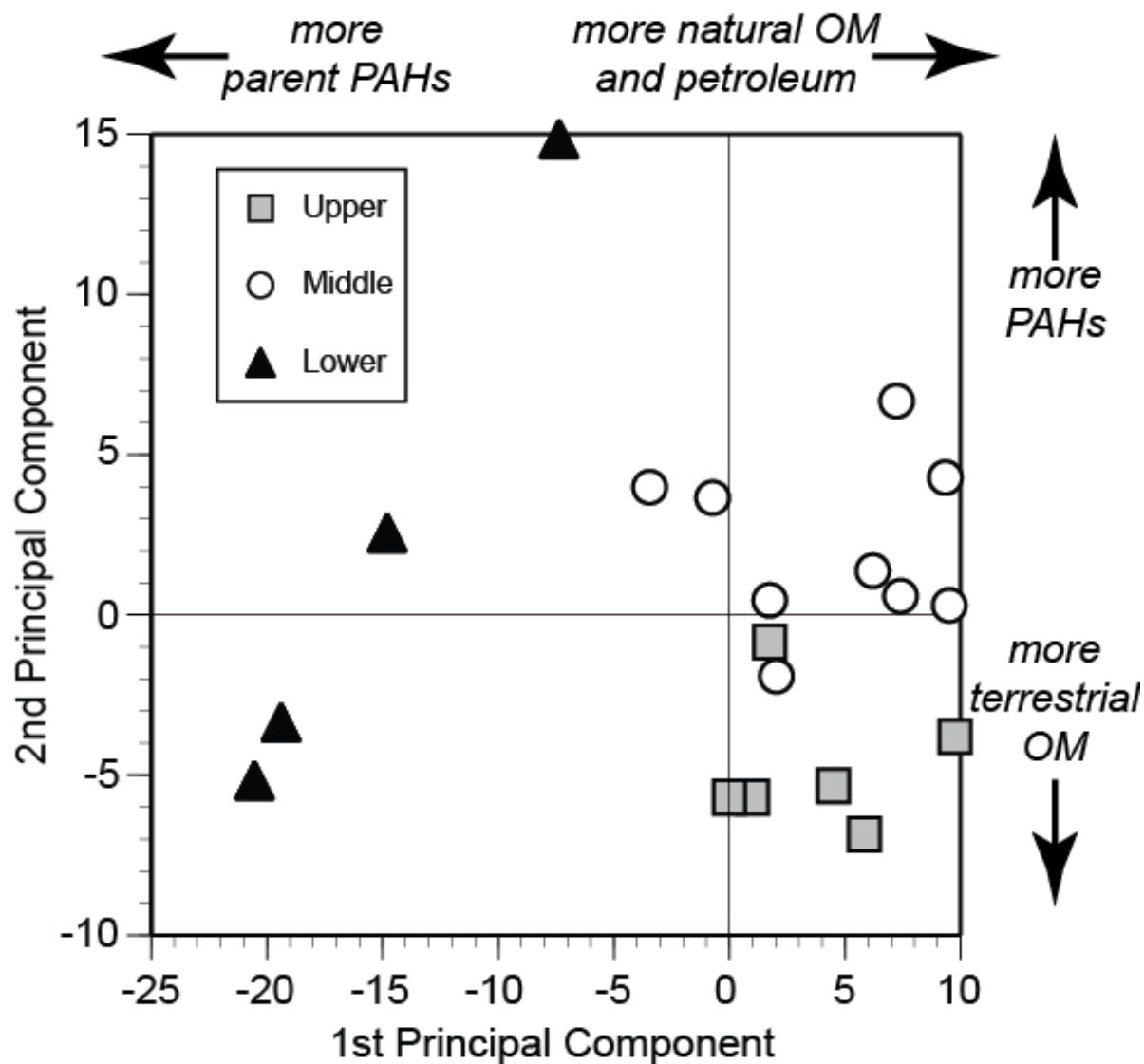


Figure 15-16. First two principal components from the multivariate analysis of the Py-GC/MS data from Lower Passaic River (New Jersey, USA) core 7A. Data input included 138 individual compounds and isomer groups from the Py-GC/MS analysis of 19 samples taken from the 5 m long sediment core. The PCA analysis indicates compositional differences between samples taken from the upper, middle and lower segments of the core and serves as an example of environmental geochemical and forensic insights that can be derived from Py-GC/MS results (data from Ref. 64).

produced upon pyrolysis of algae and bacteria [69]. Both of these compounds are frequently detected in the sediment pyrolyzates and may be quantitated using their mass spectral base peaks of  $m/z$  150 and 117, respectively. The index is computed as the simple ratio of vinylguaiacol (VG) to the sum vinylguaiacol plus indole (I) (i.e.,  $VG/(VG+I)$ ) using the  $m/z$  117 and 150 quantitation results directly, without applying mass spectral response factors [67]. End member samples, such as green algae (collected in Newark Bay, New Jersey) and pine wood have VGII values of nearly 0 and 1 respectively. As examples, sediment from Newark Bay has a low VGII of 0.34 indicating a predominance of aquatic organic matter, while a Passaic River bank sediment sample collected several kilometers upstream from Newark Bay has a higher VGII of 0.67 due to a greater terrestrial plant input (Fig. 15.17).

### 15.4.3. Pyrolytic Marker Compounds for Algal Blooms and Sewage

The particulate organic matter in suspended sediment is readily amenable to Py-GC/MS analysis [43, 70–72]. Eutrophic conditions in a Serbian tributary of the Danube River precipitated a diatom bloom. The results of the pyrolysis of the suspended particulate matter collected during this bloom [73] provide an example of the insights obtainable via this approach (Fig. 15.18). With protein-derived nitrogen compounds such as indole and methylindole (peaks N14, N15) strongly predominant over lignin marker compounds (too small to be visible on this total ion current trace), the sample has an unambiguously aquatic fingerprint and a correspondingly very low VGII of 0.01. Other distinctive compounds contributing to the algal signature include diketopiperazines (the two N18 peaks),  $C_{14}$  and  $C_{16}$  fatty acids (C1, C2, C3), phytadienes, phytol, and other isoprenoids (peaks I5-I9), and 24-methylsterenes ( $\$20$ – $\$22$ ). 24-Methylcholestadienol is a biological marker for diatoms [74] and was detected in the solvent extract of this sample. The steradienes and -trienes are the pyrolysis products of this distinctive diatom marker compound [73].

The Rock-Eval pyrolysis results for the sewage spill off the coast of Barcelona, Spain were presented in Section 15.2.1 above and in Figs. 15.3 and 15.4. The pyrolyzate of a sewage sludge sample from this site is notable for its relatively abundant organonitrogen compounds (Fig. 15.19) and a correspondingly low VGII of 0.15. Even more remarkable are the series of linear alkylbenzenes (LABs, peaks D7–D20) and steroids ( $\$1$ – $\$15$ ) on this full-scan chromatogram, useful as markers for sewage contamination of sediments [10]. In detail, the full series of  $C_{15}$ – $C_{19}$  LAB isomer groups can be seen on the  $m/z$  91 trace of this sample's pyrolyzate (Fig. 15.20). These compounds are markers for alkylbenzene sulfonate surfactants and are characteristic of urban wastewater streams. In this case, they are likely to have been thermally desorbed at the 610°C temperature employed in this experiment [10]. The sterol markers are of even greater utility in detecting sewage contamination. While the steroids are sufficiently abundant in this pyrolyzate to appear prominent on the total ion current trace (Figs.

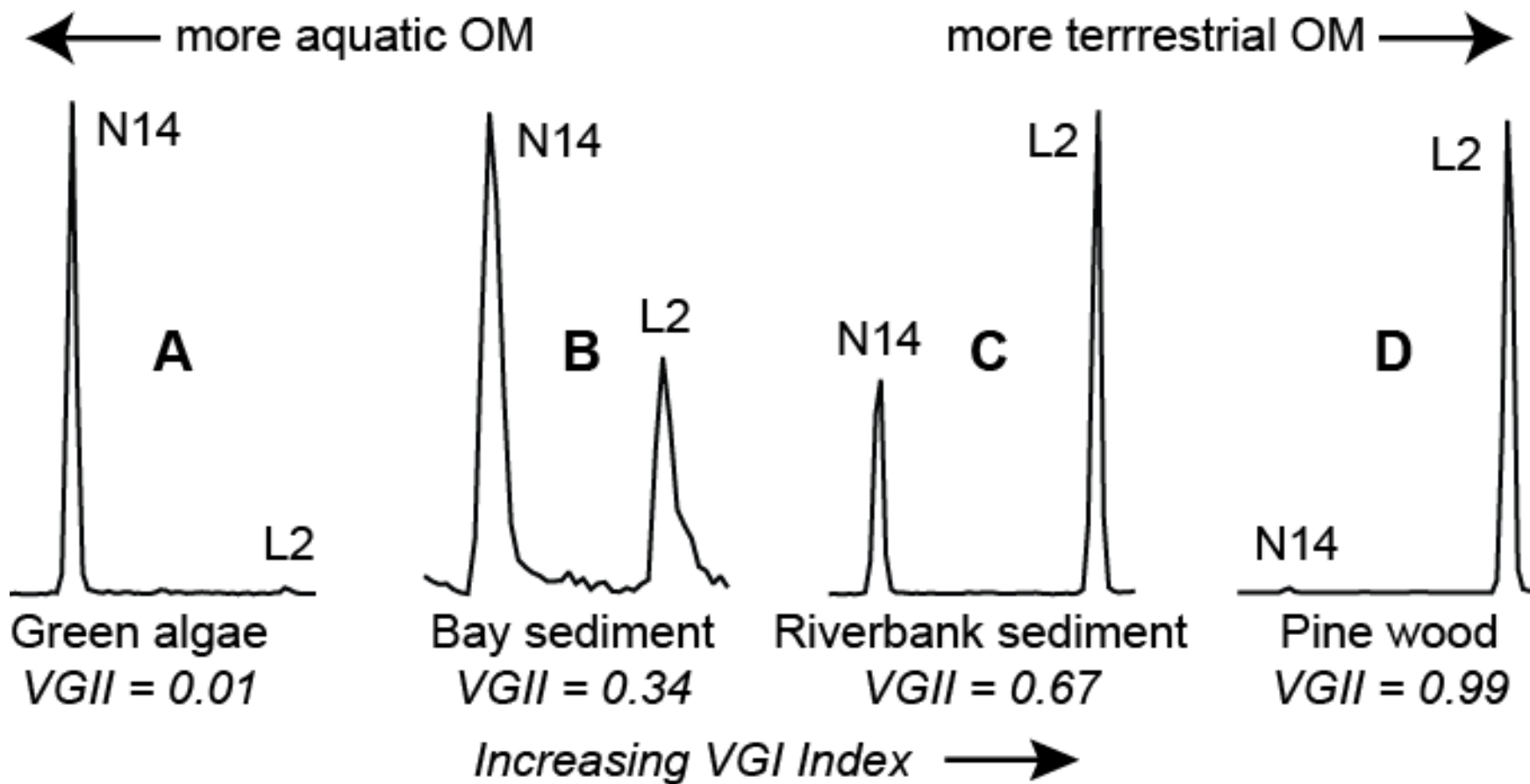


Figure 15-17. Examples of summed partial  $m/z$  117 + 150 mass chromatograms from four pyrolyzates illustrating the rationale for the Vinylguaiacol Indole Index (VGII or "Veggie" Index), which assesses the relative contributions of terrestrial and aquatic organic matter to sediments. The VGI Index increases from 0 to 1 with increasing relative amounts of terrestrial organic matter. A) Green algae (*Ulva* sp.?) from Newark Bay, New Jersey, USA representing the aquatic end member. B) Newark Bay sediment showing a predominance of aquatic organic matter. C) Passaic River (New Jersey) bank sediment with the terrestrial component predominant. D) Pine wood (*Pinus strobus* twig) representing the terrestrial end member.

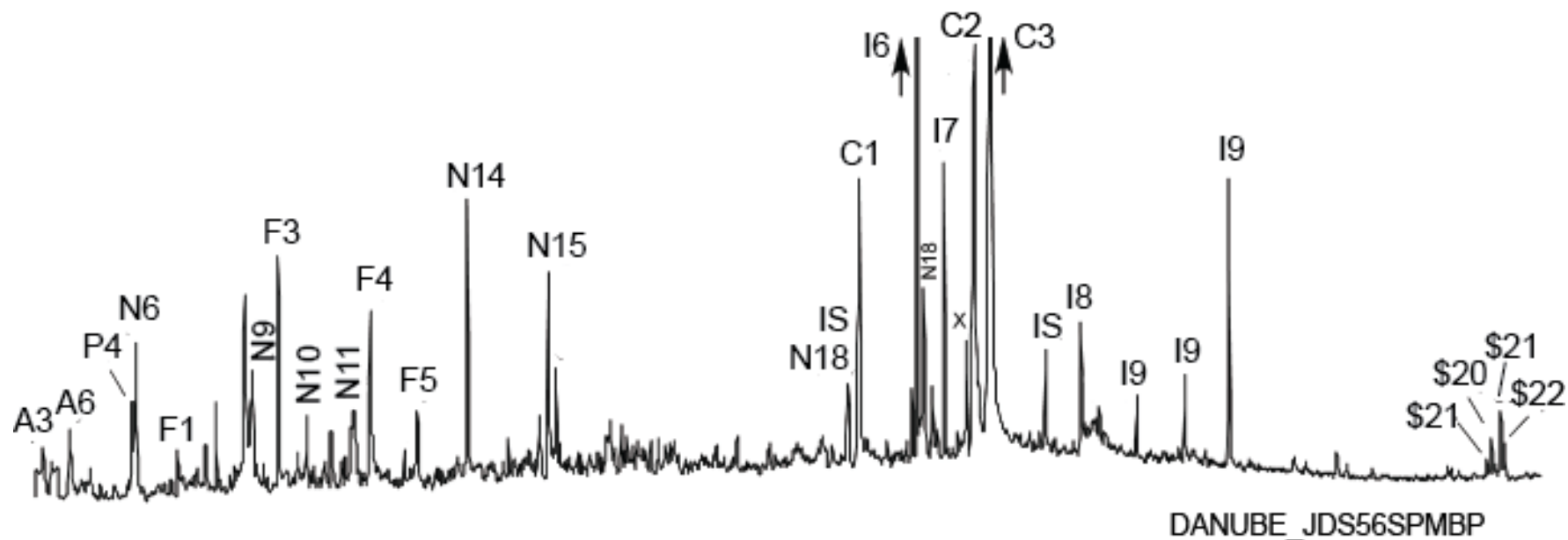


Figure 15-18. Full scan, total ion current chromatogram showing results of the pyrolysis (610 °C, 20 sec.) of suspended sediments in the Velika Morava River (Serbia), a tributary of the Danube River. See Table 1 for peak identification. The phytadienes and fatty acids provide evidence of algal blooms in the water column, likely involving diatoms, as indicated by the strong relative contributions of C28 steroids. (Adapted from Ref. 73. Used with permission.)



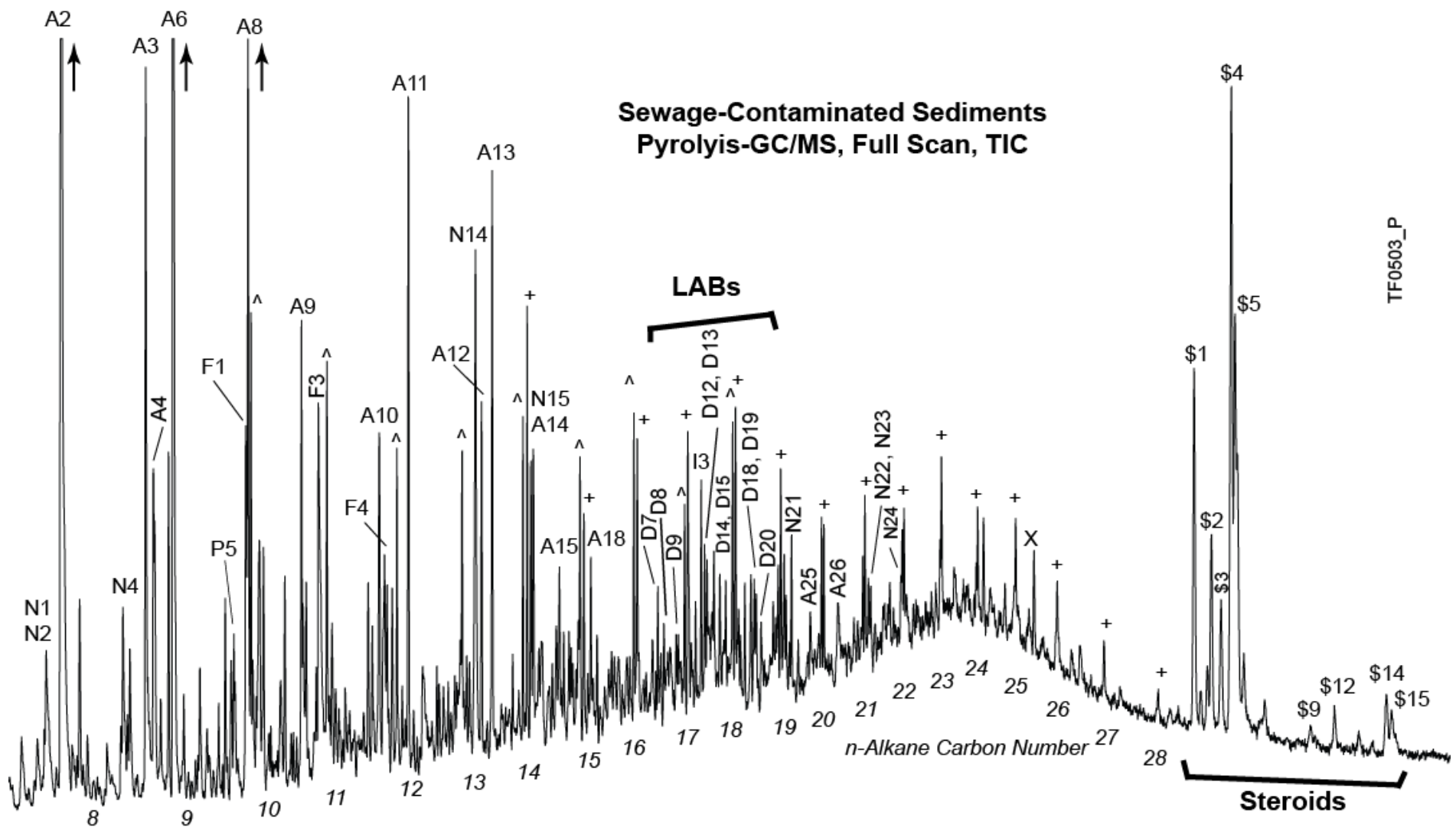


Figure 15-19. Full scan, total ion current chromatogram showing the results of the pyrolysis (610 °C, 20 sec.) of sewage sludge sampled offshore Barcelona (Spain). See Table 1 for peak identification. Note prominent linear alkyl benzenes (LABs) and sewage-related steroids. (Adapted from Ref. 10. Used with permission.)

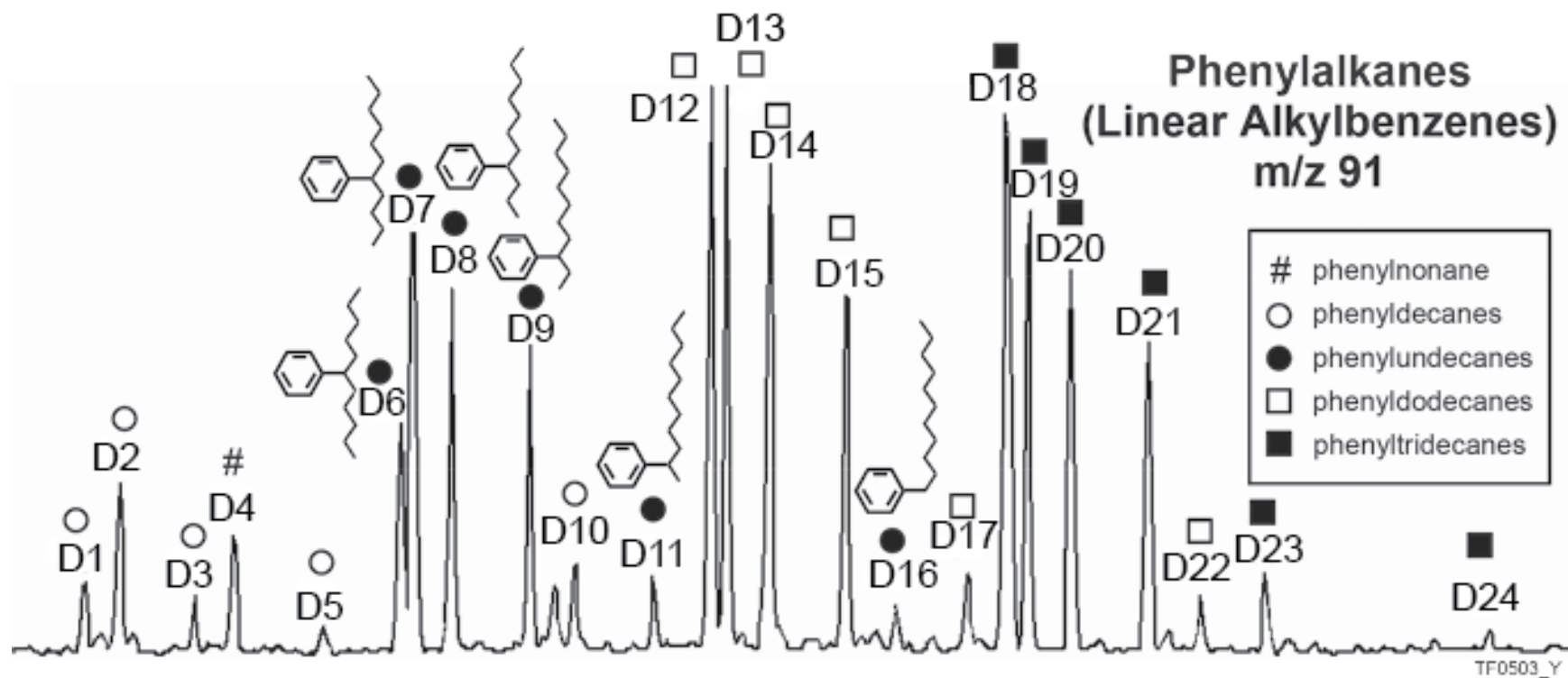


Figure 15-20. Distribution of wastewater-derived linear alkylbenzenes (LABs) as seen on a partial m/z 91 chromatogram using selected ion monitoring data from the pyrolysis (610 °C, 20 sec.) of sewage sludge of the same sample shown in Figure 15-19. (Adapted from Ref. 10. Used with permission.)

15.19 and 15.21A), mass chromatography permits an examination of their distribution in detail. Since the majority of these steroids are monounsaturated, the  $m/z$  215 trace is perhaps the most useful (Fig. 15.21B). Their molecular ions ( $m/z$  370, 384, 398, Fig. 15.21E) indicate that these are  $C_{27}$ ,  $C_{28}$ , and  $C_{29}$  sterenes and that the  $C_{27}$  are the most abundant while the  $C_{28}$  are the least. The  $C_{27}$ – $C_{29}$  steranes are also present, in about the same relative carbon number proportions as the sterenes (Fig. 15.21C). Since the  $5\alpha(H)$  (20R) stereoisomers strongly dominate in each carbon number (peaks \$5, \$11, \$15) petroleum contamination is precluded. Coprostanol is the primary sterol sewage marker and is a  $C_{27}$  compound with a molecular ion of  $m/z$  388 (Fig. 15.21D). While its minor presence in this pyrolyzate is likely due to thermodesorption, the dominant  $C_{27}$  sterenes are interpreted to be largely its pyrolysis products [10]. The  $m/z$  316, 330, and 344 fragment ions are indicative of the  $C_{27}$ – $C_{29}$  sterenes with the double bond at the C-2 position (\$2, \$3, \$8, \$9, \$13, \$14 in Fig. 15.21F).  $C_{27}$  and  $C_{29}$  steradienes are also present (Fig. 15.21G). Using this steroid distribution as a guide, particularly the  $C_{27} > C_{29} > C_{28}$  sterene pattern seen most readily on a  $m/z$  215 chromatogram, Py-GC/MS can be useful for the rapid detection of sewage contamination in sediments.

#### 15.4.4. Analytical Pyrolysis of Airborne Particulate Matter

The organic components in urban airborne particulate matter are amenable to Py-GC/MS analysis. For example, dry particulate matter from a sampling device in Lanzhou, China was pyrolyzed directly, without further preparation. The total ion current trace displays a series of  $n$ -alkanes and mono- to pentaaromatic hydrocarbons (Fig. 15.22A). The sample was reanalyzed in selected ion monitoring mode and the resulting  $n$ -alkane distribution together with the presence of norpristane, pristane and phytane (Peaks I1, I2, I5) indicate the presence of unburned fossil fuels (Fig. 15.22B). There is an odd over even  $n$ -alkane predominance in the  $C_{27}$  to  $C_{31}$  range, indicating admixed terrestrial plant waxes. The parent 2- to 5-ring PAHs are readily seen on a composite mass chromatogram constructed of their molecular ions (Fig. 15.22C). The methylphenanthrenes (A25) are also shown and since they are relatively much less abundant than the parent compound phenanthrene (A23), it is likely that the PAHs are mostly combustion-derived. Once again, the Py-GC/MS method provides a rapid means for the screening of environmental samples.

#### 15.4.5. Analytical Pyrolysis of Spilled Petroleum

In the wake of the 2010 *Deepwater Horizon* disaster in the Gulf of Mexico, large quantities of spilled oil came ashore. A relatively fresh tarball, collected within hours of landfall during the early days of the crisis, displays a partially intact series of normal and isoprenoid alkanes atop a prominent UCM hump (Fig. 15.23A). Although a pyrolysis temperature of 610°C was used for this experiment, it is likely that the yield was mostly the result of

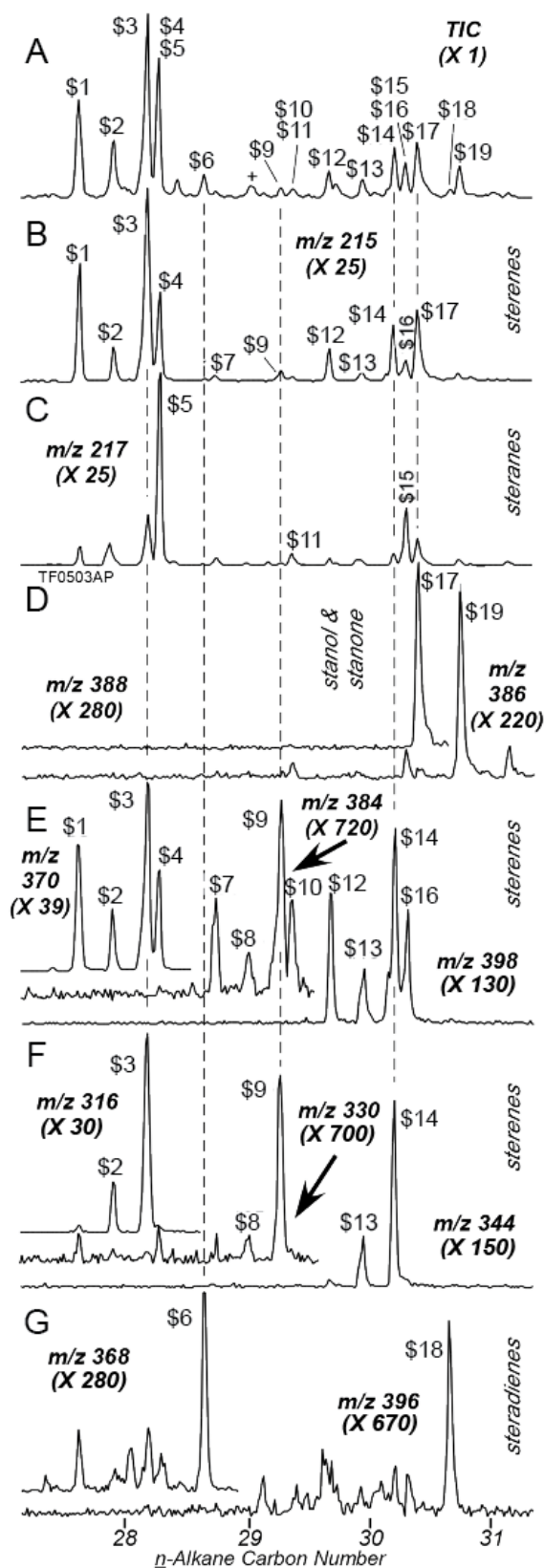


Figure 15-21. Complex distribution of sewage-derived steroids as seen on partial mass chromatograms (full scan) from the pyrolysis (610 °C, 20 sec.) of the same sample shown in Figure 15-19. Monounsaturated sterenes are the most abundant pyrolysis products, with C27 > C29 > C28. See Table 1 for peak identification. (Adapted from Ref. 10. Used with permission.)

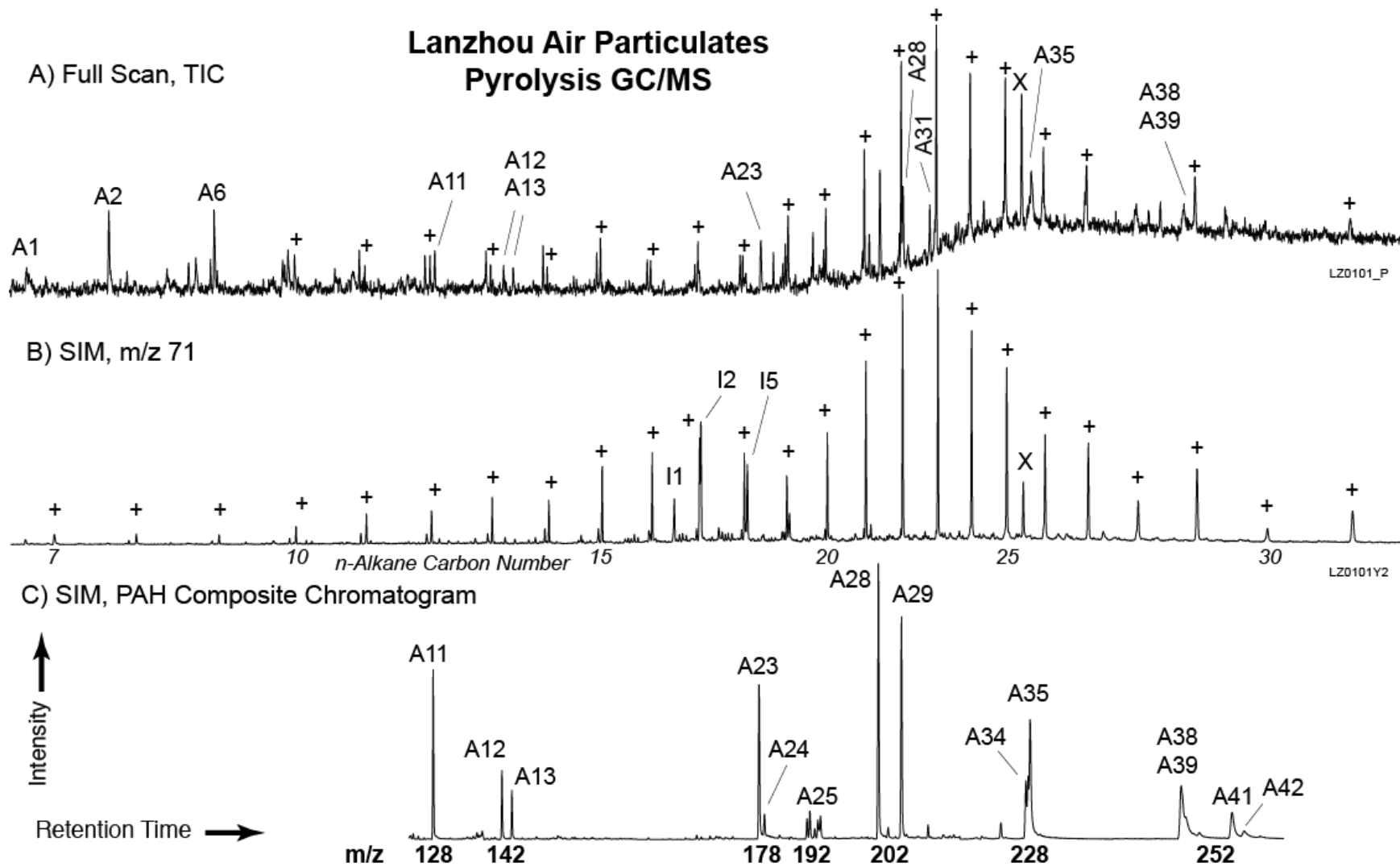
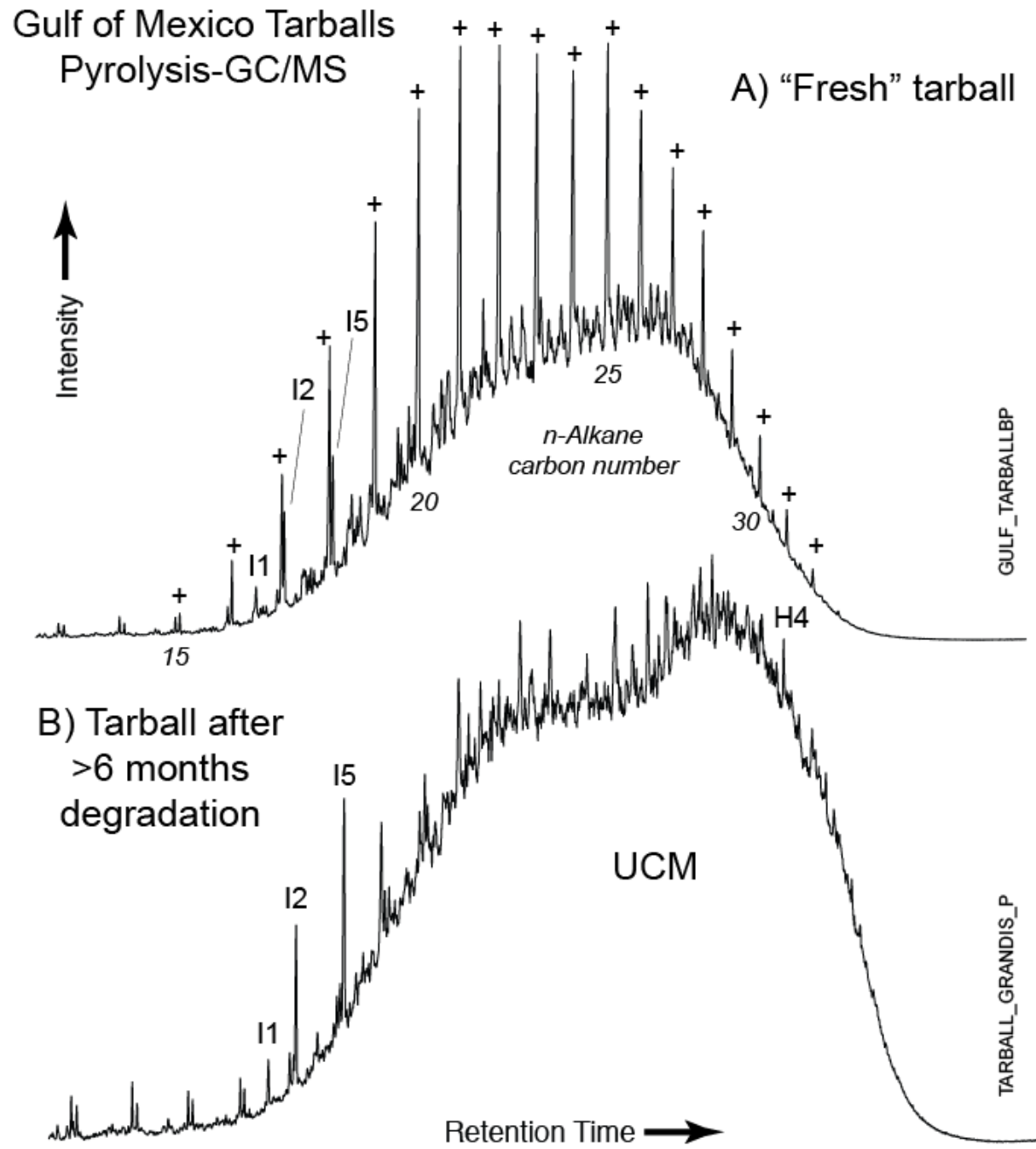


Figure 15-22. Distribution of the principal hydrocarbons detected in the pyrolyzate (610 °C, 20 sec.) of urban airborne particulate matter (Lanzhou, China). See Table 1 for peak identification. A) Total ion current trace, full scan analysis. B) m/z 71 mass chromatogram, SIM analysis. C) Composite mass chromatogram showing PAH distributions. In the composite trace, the indicated mass chromatograms are linked end-to-end, without summation or overlap.

Figure 15-23. Total ion current traces, full scan, of pyrolyzates (610 °C, 20 sec.) of beach tarballs collected on the Gulf of Mexico coast after the Deepwater Horizon disaster in 2010. See Table 1 for peak identification; note prominent hump produced by the "unresolved complex mixture" (UCM). A) "Fresh" tarball collected quickly after the spill reached the shore. B) Tarball degraded after 6 or more months of exposure on beach.



thermodesorption. The sample is obviously partly biodegraded, which occurred during its transport on marine currents from wellhead to shore. A second sample was collected after at least six months of exposure on the beach and displays a more severe degree of degradation (Fig. 15.23B). The *n*-alkanes are missing, although the isoprenoids (peaks I1, I2, I5) and hopane (H4) are still present. Relative to the fresher sample, the UCM has evidently lost some of its lower molecular weight components. Again it appears that most of the material was thermally desorbed, swamping any true pyrolysis products that may have been generated from the oil's asphaltene fraction. Analytical pyrolysis provides a novel means for the characterization of these unusual samples.

### **15.5. THERMOCHEMOLYSIS-GAS CHROMATOGRAPHY/MASS SPECTROMETRY**

In lieu of dry heating for standard thermodesorption and pyrolysis-GC/MS, the pyrolyzer may be used as a thermochemolysis reactor, in which the sample is heated in the presence of reagents, particularly tetramethylammonium hydroxide (TMAH). This reaction hydrolyzes the sample and methylates polar products yielding individual methyl esters. The products of thermochemolysis and pyrolysis experiments performed on the same samples can appear quite different [42], permitting enhanced interpretation as each method can reveal different aspects of the sample's nature.

Poerschmann and others successfully applied both conventional pyrolysis- and thermochemolysis-GC/MS to the characterization of PAH-contaminated sediment [75, 76]. Deshmukh and co-workers also applied both techniques to characterize a suite of contaminated and noncontaminated sediment samples, but found that the most interesting results illuminated the nature of the associated biogenic organic matter [77]. In a similar approach, Mansuy and others used thermochemolysis-GC/MS to evaluate the humic fraction of polluted river sediments, effectively distinguishing between natural and anthropogenic organic matter sources [78].

### **15.6. PYROLYSIS WITH OTHER DETECTION SYSTEMS**

In lieu of the standard mass spectrometer, a Py-GC system has been coupled to a combustion-isotope ratio mass spectrometer (Py-GC-C-IRMS) and used to characterize lacustrine dissolved organic matter [22]. The results of pyrolysis-FIMS (see Section 15.2.2) and Py-GC-C-IRMS of the same sample show a predominance of higher plant-derived material (Fig. 15.5). The *m/z* 44 trace (Fig. 15.5B) corresponds to the CO<sub>2</sub> produced as the eluates exiting the GC column are combusted and is functionally equivalent to a standard GC-FID chromatogram. The *m/z* 45/44 ratio trace corresponds to the <sup>13</sup>CO<sub>2</sub>/<sup>12</sup>CO<sub>2</sub> ratio of the analytes reaching the

detector, permitting the computation of the  $\delta^{13}\text{C}$  values of individual compounds, in turn permitting source inferences.

A portable pyrolysis-gas chromatography-ion mobility spectrometer (Py-GC-IMS) was designed for field deployment to detect potentially hazardous microbes in the environment with military and public safety applications<sup>79</sup>. A seldom-employed but interesting configuration combines pyrolysis with an atomic emission detector (Py-GC-AED), which can be tuned to detect elements of interest, such as carbon, as well as the heteroatoms oxygen, sulfur, nitrogen and chlorine [57]. The AED carbon channel produces results similar to an FID or full-scan total ion current MS trace, while the sulfur channel output resembles that of a sulfur-selective FPD [20, 57].

### 15.7. CONCLUSIONS

Over the past half century, analytical pyrolysis has proven itself to be an effective means for the semiquantitative characterization of complex macromolecular organic substances. It has been demonstrated that instruments such as Py-FID, Py-MS, and in particular, Py-GC/MS can provide valuable geochemical insights when applied to a wide variety of problems in environmental science. The more widespread use of analytical pyrolysis methods in the evaluation of environmental pollution is recommended, because of their relatively low cost and information-rich results.

**KEYWORDS:** Environmental Chemistry, Environmental Forensics, Contamination, Pollution, Polycyclic Aromatic Hydrocarbons (PAHs), Petroleum Spill, Sewage, Pyrolysis-Gas Chromatography/Mass Spectrometry (Py-GC/MS), Thermodesorption, Rock-Eval Pyrolysis

### REFERENCES

1. Uden, P. C. (1993). Nomenclature and Terminology for Analytical Pyrolysis (IUPAC Recommendations 1993). *Pure and Applied Chemistry*, 65(11), 2405–2409.
2. Espitalié, J., Laporte, J. L., Madec, M., Marquis, F., Leplat, P., Paulet, J., & Boutefeu, A. (1977). Méthode Rapide De Caractérisation Des Roches Mères, De Leur Potentiel Pétrolier Et De Leur Degré D'évolution, *Oil & Gas Science and Technology Rev. IFP*, 32(1), 23–42.
3. Tissot, B. P., & Welte, D. H. (1984). *Petroleum Formation and Occurrence*. 2<sup>nd</sup> Ed., Springer: 702 P.
4. Peters, K. E. (1986). Guidelines for Evaluating Petroleum Source Rock Using Programmed Pyrolysis, *AAPG Bulletin*, 70(3), 318–329.
5. Meyers, P. A., & Dose, H. (1999). Sources, Preservation, and Thermal Maturity of Organic Matter in Pliocene-Pleistocene Organic-Carbon-Rich Sediments of the Western



- Mediterranean Sea, In *Proceedings of the Ocean Drilling Program, Scientific Results*, Zahn, R., Comas, M. C., Klaus, A., Eds. 383–390.
6. Marchand, C., Lallier-Vergès, E., Disnar, J. R., & Kéravis, D. (2008). Organic Carbon Sources and Transformations in Mangrove Sediments: A Rock-Eval Pyrolysis Approach, *Organic Geochemistry*, 39, (4), 408–421.
  7. Stern, G. A., Sanei, H., Roach, P., Delaronde, J., & Outridge, P. M. (2009). Historical Interrelated Variations of Mercury and Aquatic Organic Matter in Lake Sediment Cores from a Subarctic Lake in Yukon, Canada: Further Evidence Toward the Algal-Mercury Scavenging Hypothesis, *Environmental Science & Technology*, 43(20), 7684–7690.
  8. Duan, D., Ran, Y., Cheng, H., Chen, J. A., & Wan, G., Contamination Trends of Trace Metals and Coupling with Algal Productivity in Sediment Cores in Pearl River Delta, South China, *Chemosphere*, (In Press).
  9. Kruge, M. A., Mukhopadhyay, P. K., & Lewis, C. F. M. (1998). A Molecular Evaluation of Contaminants and Natural Organic Matter in Bottom Sediments from Western Lake Ontario. *Organic Geochemistry*, 29(5–7), 1797–1812.
  10. Kruge, M. A., Permanyer, A., Serra, J., & Yu, D. (2010). Geochemical Investigation of An Offshore Sewage Sludge Deposit, Barcelona, Catalonia, Spain. *Journal of Analytical and Applied Pyrolysis*, 89(2), 204–217.
  11. Maddock, C. J., & Ottley, T. W. (2007). Pyrolysis Mass Spectrometry: Instrumentation, Techniques, and Applications. in *Applied Pyrolysis Handbook*, 2 Ed., Wampler, T. P., Ed. CRC Press: Boca Raton, 47–64.
  12. Gutteridge, C. S., & Norris, J. R. (1979). The Application of Pyrolysis Techniques to the Identification of Micro-Organisms. *Journal of Applied Bacteriology*, 47(1), 5–43.
  13. Meuzelaar, H. L., Windig, W., Harper, A. M., Huff, S. M., McClellenn, W. H., & Richards, J. M. (1984). Pyrolysis Mass Spectrometry of Complex Organic Materials. *Science*, 226, 268–274.
  14. Boon, J. J., Tom, A., Brandt, B., Eijkel, G. B., Kistemaker, P. G., Notten, F. J. W., & Mikx, F. H. M. (1984). Mass Spectrometric and Factor Discriminant Analysis of Complex Organic Matter from the Bacterial Culture Environment of *Bacteroides Gingivalis*. *Analytica Chimica Acta*, 163(0), 193–205.
  15. Ford, T., Sacco, E., Black, J., Kelley, T., Goodacre, R., Berkeley, R. C., & Mitchell, R. (1991). Characterization of Exopolymers of Aquatic Bacteria by Pyrolysis Mass Spectrometry, *Applied and Environmental Microbiology*, 57(6), 1595–1601.
  16. Goodacre, R., Shann, B., Gilbert, R. J., Timmins, É. M., McGovern, A. C., Alsberg, B. K., Kell, D. B., & Logan, N. A. (2000). Detection of the Dipicolinic Acid Biomarker in *Bacillus* Spores Using Curie-Point Pyrolysis Mass Spectrometry and Fourier Transform Infrared Spectroscopy, *Analytical Chemistry*, 72(1), 119–127.

17. Qian, K., Killinger, W. E., Casey, M., & Nicol, G. R. (1996). Rapid Polymer Identification by In-Source Direct Pyrolysis Mass Spectrometry and Library Searching Techniques, *Analytical Chemistry*, 68(6), 1019–1027.
18. Boon, J. J., Dupont, L., & De Leeuw, J. W. (1986). Characterization of a Peat Bog Profile by Curie Point Pyrolysis-Mass Spectrometry Combined with Multivariate Analysis and by Pyrolysis Gas Chromatography-Mass Spectrometry, In *Peat and Water*, Fuchsman, C. H., Ed. Elsevier: 215–239.
19. Remmler, M., Kopinke, F. D., & Stottmeister, U. (1995). Thermoanalytical Methods for Characterizing Hydrocarbon-Sludge-Soil Mixtures, *Thermochimica Acta*, 263, 101–112.
20. Pörschmann, J., Kopinke, F. D., Remmler, M., Mackenzie, K., Geyer, W., & Mothes, S. (1996). Hyphenated Techniques for Characterizing Coal Wastewaters and Associated Sediments, *Journal of Chromatography A*, 750(1–2), 287–301.
21. Miketova, P., Abbas-Hawks, C., Voorhees, K. J., & Hadfield, T. L. (2003). Microorganism Gram-Type Differentiation of Whole Cells Based on Pyrolysis High-Resolution Mass Spectrometry Data, *Journal of Analytical and Applied Pyrolysis*, 67(1), 109–122.
22. Schulten, H. R., & Gleixner, G. (1999). Analytical Pyrolysis of Humic Substances and Dissolved Organic Matter in Aquatic Systems: Structure and Origin. *Water Research*, 33(11), 2489–2498.
23. Schulten, H. R. (1999). Analytical Pyrolysis and Computational Chemistry of Aquatic Humic Substance and Dissolved Organic Matter, *Journal of Analytical and Applied Pyrolysis*, 49, 385–415.
24. Leinweber, P., & Schulten, H. R. (1999). Advances in Analytical Pyrolysis of Soil Organic Matter, *Journal of Analytical and Applied Pyrolysis*, 49(1–2), 359–383.
25. Letarte, S., Morency, D., Wilkes, J., & Bertrand, M. J. (2004). Py-MAB-Tof Detection and Identification of Microorganisms in Urine. *Journal of Analytical and Applied Pyrolysis*, 71(1), 13–25.
26. Jeannotte, R., Hamel, C., Jabaji, S., & Whalen, J. K. (2011). Pyrolysis-Mass Spectrometry and Gas Chromatography-Flame Ionization Detection as Complementary Tools for Soil Lipid Characterization, *Journal of Analytical and Applied Pyrolysis*, 90(2), 232–237.
27. Getty, S. A., Ten Kate, I. L., Feng, S. H., Brinckerhoff, W. B., Cardiff, E. H., Holmes, V. E., King, T. T., Li, M. J., Mumm, E., Mahaffy, P. R., & Glavin, D. P. (2010). Development of an Evolved Gas-Time-of-Flight Mass Spectrometer for the Volatile Analysis by Pyrolysis of Regolith (Vapor) Instrument, *International Journal of Mass Spectrometry*, 295(3), 124–132.
28. Wampler, T. P. (2007). Analytical Pyrolysis: An Overview, In *Applied Pyrolysis Handbook*, 2, Ed., Wampler, T. P., Ed. CRC Press: Boca Raton, 1–26.
29. Wampler, T. P. (2007). Instrumentation and Analysis. In *Applied Pyrolysis Handbook*, 2, Ed., Wampler, T. P., Ed. CRC Press: Boca Raton, 27–46.

30. Jones, C. E. R. (2000). Gas Chromatography: Pyrolysis Gas Chromatography, In *Encyclopedia of Separation Science*, Wilson, I. D., Adlard, E. R., Cooke, M., & Poole, C. F., Eds. Academic Press: 282–287.
31. Davison, W. H. T., Slaney, S., & Wragg, A. L. (1954). A Novel Method of Identification of Polymers, *Chemistry and Industry*, 1356.
32. Giraud, A. (1970). Application of Pyrolysis and Gas Chromatography to Geochemical Characterization of Kerogen in Sedimentary Rock, *AAPG Bulletin*, 54, (3), 439–455.
33. Irwin, W. J. (1979). Analytical Pyrolysis An Overview, *Journal of Analytical and Applied Pyrolysis*, 1(1), 3–25.
34. Dembicki, H., Horsfield, B., & Ho, T. T. Y. (1983). Source Rock Evaluation by Pyrolysis-Gas Chromatography, *AAPG Bulletin*, 67(7), 1094–1103.
35. Whelan, J. K., Hunt, J. M., & Huc, A. Y. (1980). Applications of Thermal Distillation-Pyrolysis to Petroleum Source Rock Studies and Marine Pollution, *Journal of Analytical and Applied Pyrolysis*, 2(1), 79–96.
36. Hala, W. W. (1993). Organic Geochemistry of Contaminated Soil from an Abandoned Oil Field. MS Thesis. Southern Illinois University, Carbondale, .
37. Gallegos, E. J. (1975). Terpane-Sterane Release from Kerogen by Pyrolysis Gas Chromatography-Mass Spectrometry. *Analytical Chemistry*, 47(9), 1524–1528.
38. De Leeuw, J. W., De Leer, E. W. B., Damste, J. S. S., & Schuyf, P. J. W. (1986). Screening of Anthropogenic Compounds in Polluted Sediments and Soils by Flash Evaporation/Pyrolysis Gas Chromatography Mass Spectrometry, *Analytical Chemistry*, 58(8), 1852–1857.
39. White, D. M., Garland, D. S., Beyer, L., & Yoshikawa, K. (2004). Pyrolysis-GC/MS Fingerprinting of Environmental Samples, *Journal of Analytical and Applied Pyrolysis*, 71(1), 107–118.
40. Saiz-Jimenez, C., Grimalt, J., Garcia-Rowe, J., & Ortega-Calvo, J. J. (1991). Analytical Pyrolysis of Lichen Thalli, *Symbiosis*, 11, 313–326.
41. Saiz-Jimenez, C. (1992). Applications of Pyrolysis-Gas Chromatography/Mass Spectrometry to the Study of Soils, Plant Materials and Humic Substances, A Critical Appraisal, In *Humus, Its Structure and Role in Agriculture and Environment*, Kubát, J., Ed. Elsevier: 27–38.
42. Saiz-Jimenez, C. (1994). Analytical Pyrolysis of Humic Substances: Pitfalls, Limitations, and Possible Solutions, *Environmental Science & Technology*, 28(11), 1773–1780.
43. Van Heemst, J. D. H., Van Bergen, P. F., Stankiewicz, B. A., & De Leeuw, J. W. (1999). Multiple Sources of Alkylphenols Produced Upon Pyrolysis of DOM, POM and Recent Sediments, *Journal of Analytical and Applied Pyrolysis*, 52(2), 239–256.

44. Richnow, H. H., Seifert, R., Kästner, M., Mahro, B., Horsfield, B., Tiedgen, U., Böhm, S., & Michaelis, W. (1995). Rapid Screening of PAH-Residues in Bioremediated Soils, *Chemosphere*, *31*(8), 3991–3999.
45. Schiavon, N., Chiavari, G., Schiavon, G., & Fabbri, D. (1995). Nature and Decay Effects of Urban Soiling on Granitic Building Stones, *Science of the Total Environment*, *167*(1–3), 87–101.
46. Schmidt, M. W. I., Knicker, H., Hatcher, P. G., & Kögel-Knabner, I. (1996). Impact of Brown Coal Dust on the Organic Matter in Particle-Size Fractions of a Mollisol, *Organic Geochemistry*, *25*(1–2), 29–39.
47. Abdel Bagi, S. T. (1996). Geochemical and Petrographical Characterization of Natural and Anthropogenic Sedimentary Organic Matter in Polluted Sediments from the West Branch of the Grand Calumet River and Roxana Marsh, NW Indiana and NE Illinois, PhD Dissertation, Southern Illinois University, Carbondale.
48. Kim, M. G., Yagawa, K., Inoue, H., & Shirai, T. (1991). Determination of Sulfates in Urban Air by Pyrolysis Gas Chromatography with Flame Photometric Detection, *Journal of Analytical and Applied Pyrolysis*, *20*(0), 263–273.
49. Munson, T. O. (2007). Environmental Applications of Pyrolysis. In *Applied Pyrolysis Handbook*, 2, Wampler, T. P., Ed. CRC Press: Boca Raton, 133–173.
50. Fabbri, D., Trombini, C., & Vassura, I. (1998). Analysis of Polystyrene in Polluted Sediments by Pyrolysis Gas Chromatography Mass Spectrometry, *Journal of Chromatographic Science*, *36*, 600–604.
51. Fabbri, D., Tartari, D., & Trombini, C. (2000). Analysis of Poly(Vinyl Chloride) and Other Polymers in Sediments and Suspended Matter of a Coastal Lagoon by Pyrolysis Gas Chromatography Mass Spectrometry, *Analytica Chimica Acta*, *413*(1–2), 3–11.
52. Fabbri, D. (2001). Use of Pyrolysis-Gas Chromatography/Mass Spectrometry to Study Environmental Pollution Caused by Synthetic Polymers: A Case Study: The Ravenna Lagoon, *Journal of Analytical and Applied Pyrolysis*, *58–59*(0), 361–370.
53. Moldoveanu, S. C. (2005). *Analytical Pyrolysis of Synthetic Organic Polymers*. Elsevier, 714.
54. Kusch, P. (2012). Pyrolysis-Gas Chromatography/Mass Spectrometry of Polymeric Materials, In *Advanced Gas Chromatography Progress in Agricultural, Biomedical and Industrial Applications*, Mohd, M. A., Ed. Intech, 343–362.
55. Kruge, M. A., & Permanyer, A. (2004). Application of Pyrolysis GC/MS for Rapid Assessment of Organic contamination in Sediments from Barcelona Harbor, *Organic Geochemistry*, *35*(11–12), 1395–1408.

56. Faure, P., & Landais, P. (2001). Rapid Contamination Screening of River Sediments by Flash Pyrolysis–Gas Chromatography Mass Spectrometry (Pygc–MS) and Thermodesorption GC–MS (Tdgc–MS). *Journal of Analytical and Applied Pyrolysis*, 57(2), 187–202.
57. Faure, P., Vilmin, F., Michels, R., Jarde, E., Mansuy, L., Elie, M., & Landais, P. (2002). Application of Thermodesorption and Pyrolysis–GC–AED to the Analysis of River Sediments and Sewage Sludges for Environmental Purpose, *Journal of Analytical and Applied Pyrolysis*, 62(2), 297–318.
58. USEPA, Semivolatile Organic Compounds (Pahs and Pcb) in Soils/Sludges and Solid Wastes using Thermal Extraction/Gas Chromatography/Mass Spectrometry (TE/GC/MS). EPA Method 8275A. 1996, 23 P.
59. Stout, S. A., & Wang, Z. (2007). Chemical Fingerprinting of Spilled or Discharged Petroleum Methods and Factors Affecting Petroleum Fingerprints in the Environment, In *Oil Spill Environmental Forensics*, Wang, Z., Stout, S. A., Eds. Elsevier: Amsterdam, 1–53.
60. Douglas, G. S., Stout, S. A., Uhler, A. D., Mccarthy, K. J., & Emsbo-Mattingly, S. D. (2007). Advantages of Quantitative Chemical Fingerprinting in Oil Spill Source Identification, In *Oil Spill Environmental Forensics*, Wang, Z., Stout, S. A., Eds. Elsevier: Amsterdam, 257–292.
61. Bucu, S., Moragues, M., Doumenq, P., Noor, A., & Mille, G. (2004). Analysis of Polycyclic Aromatic Hydrocarbons in Contaminated Soil by Curie Point Pyrolysis Coupled to Gas Chromatography Mass Spectrometry, an Alternative to Conventional Methods, *Journal of Chromatography A*, 1026(1–2), 223–229.
62. Stout, S. A., Uhler, A. D., & Mccarthy, K. J. (2001). A Strategy and Methodology for Defensibly Correlating Spilled Oil to Source Candidates, *Environmental Forensics*, 2, 87–98.
63. Mudge, S. M. (2007). Multivariate Statistical Methods in Environmental Forensics, *Environmental Forensics*, 8(1–2), 155–163.
64. Bujalski, N. M. (2010). Characterization of Contaminant and Biomass Derived Organic Matter in Sediments from the Lower Passaic River, New Jersey, USA. MS Thesis, Montclair State University, Montclair (NJ).
65. Meyers, P. A. (1997). Organic Geochemical Proxies of Paleoceanographic, Paleolimnologic, and Paleoclimatic Processes, *Organic Geochemistry*, 27(5–6), 213–250.
66. Twichell, S. C., Meyers, P. A., & Diester-Haass, L. (2002). Significance of High C/N Ratios in Organic-Carbon-Rich Neogene Sediments under the Benguela Current Upwelling System, *Organic Geochemistry*, 33(7), 715–722.
67. Micić, V., Kruge, M., Körner, P., Bujalski, N., & Hofmann, T. (2010). Organic Geochemistry of Danube River Sediments from Pančevo (Serbia) to the Iron Gate Dam (Serbia–Romania), *Organic Geochemistry*, 41(9), 971–974.

68. Saiz-Jimenez, C., & De Leeuw, J. W. (1986). Lignin Pyrolysis Products: their Structures and their Significance as Biomarkers, *Organic Geochemistry*, *10(4–6)*, 869–876.
69. Bennett, B., Lager, A., Russell, C. A., Love, G. D., & Larter, S. R. (2004). Hydropyrolysis of Algae, Bacteria, Archaea and Lake Sediments; Insights into the Origin of Nitrogen Compounds in Petroleum, *Organic Geochemistry*, *35(11–12)*, 1427–1439.
70. Çoban-Yildiz, Y., Chiavari, G., Fabbri, D., Gaines, A. F., Galletti, G., & Tuğrul, S. (2000). The Chemical Composition of Black Sea Suspended Particulate Organic Matter: Pyrolysis-GC/MS as a Complementary Tool to Traditional Oceanographic Analyses, *Marine Chemistry*, *69(1–2)*, 55–67.
71. Çoban-Yildiz, Y., Fabbri, D., Tartari, D., Tuğrul, S., & Gaines, A. F. (2000). Application of Pyrolysis–GC/MS for the Characterisation of Suspended Particulate Organic Matter in the Mediterranean Sea: A Comparison with the Black Sea, *Organic Geochemistry*, *31(12)*, 1627–1639.
72. Çoban-Yildiz, Y., Fabbri, D., Baravelli, V., Vassura, I., Yilmaz, A., Tuğrul, S., & Eker-Develi, E. (2006). Analytical Pyrolysis of Suspended Particulate Organic Matter from the Black Sea Water Column, *Deep Sea Research Part II: Topical Studies in Oceanography*, *53(17–19)*, 1856–1874.
73. Micić, V., Kruge, M. A., Köster, J., & Hofmann, T. (2011). Natural, Anthropogenic and Fossil Organic Matter in River Sediments and Suspended Particulate Matter: a Multi-Molecular Marker, Approach. *Science of the Total Environment*, *409(5)*, 905–919.
74. Rampen, S. W., Abbas, B. A. S. S., & Sinninghe Damsté, J. S. (2010). A Comprehensive Study of Sterols in Marine Diatoms (Bacillariophyta): Implications for their use as Tracers for Diatom Productivity, *Limnology and Oceanography*, *55*, 91–105.
75. Poerschmann, J., Parsi, Z., & Gorecki, T. (2008). Non-Discriminating Flash Pyrolysis and Thermochemolysis of Heavily Contaminated Sediments from the Hamilton Harbor (Canada), *Journal of Chromatography A*, *1186(1–2)*, 211–221.
76. Poerschmann, J., Trommler, U., Fabbri, D., & Górecki, T. (2007). Combined Application of Non-Discriminated Conventional Pyrolysis and Tetramethylammonium Hydroxide-Induced Thermochemolysis for the Characterization of the Molecular Structure of Humic Acid Isolated from Polluted Sediments from the Ravenna Lagoon, *Chemosphere*, *70(2)*, 196–205.
77. Deshmukh, A. P., Chefetz, B., & Hatcher, P. G. (2001). Characterization of Organic Matter in Pristine and Contaminated Coastal Marine Sediments using Solid-State <sup>13</sup>C NMR, Pyrolytic and Thermochemolytic Methods: A Case Study in the San Diego Harbor Area, *Chemosphere*, *45(6–7)*, 1007–1022.
78. Mansuy, L., Bourezgui, Y., Garnier-Zarli, E., Jardé, E., & Réveillé, V. (2001). Characterization of Humic Substances in Highly Polluted River Sediments by Pyrolysis

Methylation Gas Chromatography Mass Spectrometry, *Organic Geochemistry*, 32(2), 223–231.

79. Snyder, A. P., Dworzanski, J. P., Tripathi, A., Maswadeh, W. M., & Wick, C. H. (2004). Correlation of Mass Spectrometry Identified Bacterial Biomarkers from a Fielded Pyrolysis Gas Chromatography Ion Mobility Spectrometry Biodetector with the Microbiological Gram Stain Classification Scheme, *Analytical Chemistry*, 76(21), 6492–6499.